Genetic Analysis of F1 Cluster Phages that Infect *Mycobacterium smegmatis* Identifies Two Distinct Holin-Like Proteins that Regulate the Host Lysis Event

Running Title: Two Distinct Phage Holin Proteins Regulate the Host Lysis Event in *M. smegmatis*

Richard S. Pollenz[a#], Kira Ruiz-Houston[b], Wynter Dean[a] and Loc Nguyen[a]

[a]Department of Molecular Bioscience, University of South Florida, Tampa, FL

[b]Department of Microbiology, University of Wisconsin, Madison, WI

[#]Corresponding Author:

Richard S Pollenz

Department of Molecular Biosciences

University of South Florida

4202 E Fowler Ave ISA2015

Tampa, FL 33620

pollenz@usf.edu

813-767-3984

ABSTRACT

Phages Girr and NormanBulbieJr (NBJ) infect Gram-positive *Mycobacterium smegmatis* mc^2 155. Both phages contain conserved lysis cassettes that harbor two endolysin genes (*lysin A* and *lysin B*) and two genes encoding transmembrane domain (TMD) holin-like proteins. The first holin-like protein, termed LysF1a is 88 amino acids, has two TMDs and a predicted N-in-C-in membrane topology. The second, termed LysF1b, has a single N-terminal TMD and a predicted N-out-C-in topology making it distinct from the 1TMD type III holins or spanins in size and membrane topology. Deletion of either *lysF1a* or *lysF1b* results in lysis defect phenotypes manifest by reduced plaque size and changes to lysis timing in liquid culture. Deletion of both *lysF1a* and *lysF1b* genes is lethal to phage propagation supporting holin function. Phages expressing only the LysF1b protein trigger lysis prematurely when exposed to energy poisons while phages expressing only LysF1a do not show early triggering. Lysis recovery mutants were isolated from phages lacking the *lysF1b* gene and these mutants generated wild type plaque size but triggered lysis prematurely and showed ~65% reductions in burst size. Genome sequencing identified different point mutations that mapped to TMD1 or the C-terminal region of the *lysF1a* gene. Finally, infection of an *M. smegmatis* strain that does not produce lipomannan and lipoarabinomannan by either wild type phages or phages carrying the *lysF1b* deletion showed modest plaque size increases and did not fully complement the lysis defect of phages lacking the *lysF1b* gene. Collectively, the findings show that both LysF1a and LysF1b function as holins and are required for efficient bacterial lysis. LysF1a does not function as an antiholin but requires the expression of the LysF1b protein for efficient lysis functioning. The requirement of two holins with distinct membrane topologies for host lysis has not been described previously.

43 **INTRODUCTION**

44 With an estimated 10^{31} different bacteriophage particles in the world, the pathway
45 whereby dsDNA phages lyse their bacterial hosts after infection and replication is one of the
46 most common cell fates on earth [1]. Extensive biochemical and genetic work with dsDNA
47 phages that infect Gram-negative hosts has established a general three-step model for the
48 triggering of the lysis pathway that involves three distinct sets of proteins. The first are
49 endolysin/s that have defined catalytic activity to lyse the peptidoglycan (PG) layer [2]. The
50 second are holin or antiholin proteins that have between 1-4 transmembrane domain helices
51 (TMD). These proteins work together to, 1) control the timing of the lysis event following phage
52 infection [3, 4], 2) assist with the destabilization of the membrane proton motive force (PMF) [3,
53 4] and 3) in the canonical holin models, generate large 1μm "pores" in the inner membrane (IM)
54 to allow the exit of the endolysin enzymes to the periplasmic space where they can access and
55 cleave the PG layer [5, 6]. Finally, there are secreted membrane proteins and lipoproteins
56 termed spanins that are associated with the IM and outer membrane (OM). There proteins
57 interact after the PG layer is cleaved to generates the lesion across the IM and OM that allows
58 for the efficient release of the phage progeny [7-9].

59 dsDNA phages such as lambda, P2, and phage 21 all have genomes < 50,00bp and
60 have a clustered lysis cassette that contain all the genes necessary to mediate the bacterial
61 lysis event [10-12]. Phage lambda encodes the canonical type I holin protein that has 3TMDs
62 and forms large oligomers that create 1μm holes in the IM to allow exit of the endolysin from the
63 cytoplasm to the periplasmic space [12]. Phage 21 defines the type II pinholin lysis pathway and
64 utilizes a 2TMD holin protein that forms ~1,000 heptamers in the IM. The pinholins create only
65 nanometer size holes that are not big enough to allow exit of the endolysin, and they function to
66 disrupt the PMF and trigger lysis. Thus, phages that encode pinholins also encode endolysins
67 that carry secretion-arrest-release (SAR) signals and the SAR-endolysin is held in an inactive

68 state in the IM prior to triggering. The disruption of the PMF causes the release of the IM
69 tethered SAR-endolysin to the periplasmic space where it cleaves the PG [4, 13, 14]. In both
70 lambda and phage 21, a single open reading frame with two in-frame start codons (dual start
71 motif) encodes two holin proteins that only differ by the addition of 1-2 N-terminal amino acids
72 [10, 11, 14, 15]. The longer version of each holin functions as the inactive antiholin and in both
73 cases a percentage of the holin forms dimers with the antiholin that holds that holin in an
74 inactive state prior to triggering. Upon triggering, the antiholin assumes active holin function
75 greatly increasing the amount of active holin protein available for hole formation. In phages with
76 large genomes, such as P1 and T4, the holin, antiholin, endolysin and spanin genes can be
77 bioinformatically characterized throughout the genome and are not in a defined cassette. The
78 type III holin from phage T4 has a single N-terminal TMD with an N-in-C-out topology with the
79 bulk of the sequence oriented in the periplasmic space [16, 17]. T4 phage encodes two different
80 antiholin proteins that modulate the holin lysis timing and participate in the lysis inhibition activity
81 of phage T4 [16, 17]. Thus, a common theme in the phage-mediated lysis pathway of lambda,
82 P1, P2 and T4 is the utilization of holins and antiholins to regulate the lysis event. However,
83 another variation of the lysis pathway has recently been shown for the Enterococcal phage Mu
84 [18]. Mu does not utilize canonical holins and antiholins in the bacterial lysis pathway and
85 instead uses a novel 1TMD protein termed a releasin protein to release the SAR-endolysin from
86 the IM so it can cleave the PG [18]. As with lambda and phage 21, Mu contains canonical
87 spanins to create the final lesion for progeny release once the PG has been cleaved. It is
88 speculated that Mu does not utilize the holin/antiholin regulated lysis mechanism because it
89 copies its genome via replicative transposition during the lytic cycle and has less selective
90 pressure due to transposition immunity [18]. This pathway adds yet another variation in phage-
91 mediated bacterial lysis and it is striking that all the *E. coli* phages that have been rigorously
92 studied utilize a similar set of tools to complete the lysis pathway through distinct molecular
93 mechanisms.

94 There are 1000s of annotated dsDNA phages that infect Gram-positive hosts, yet the
95 molecular mechanism that these pages use to lyse their hosts is not resolved to the level of the
96 *E. coli* phages. Although it is hypothesized that the lysis mechanism in these phages will utilize
97 a similar set of proteins as described for phages that infect Gram-negative bacteria, the bulk of
98 biochemical and genetic work has focused more on the enzymes that target the cell wall than on
99 the holins, possibly because these enzymes may be employed as antibiotic agents [19-21].
100 Gram-positive bacteria lack a formal OM and instead have a much more complex PG layer and
101 an extended structural cell wall components beyond the PG such as arabinogalactans and
102 mycolic acids [22-25]. Thus, addition of an endolysin to Gram-positive bacteria can result in cell
103 death. Bioinformatic, biochemical and genetic analysis has identified several types of phage-
104 encoded endolysins that target different regions of the cell wall. The first type of endolysin is
105 termed lysin A and targets distinct domains of the peptidoglycan [20, 26]. These enzymes are
106 highly modular, do not contain canonical SAR domains, and deletion studies show that the lysin
107 A is essential to phage propagation [27, 28]. It is unknown if the lysin A is released to the
108 peptidoglycan layer through holins since some studies show that exogenous expression of
109 selected lysin A enzymes can be cytotoxic to *M. smegmatis* [20, 29-32]. Many phages that infect
110 Gram-positive hosts also contain a second endolysin termed lysin B that targets the linkages in
111 the mycolic acid layer of the cell wall [27, 30, 33, 34]. It has been hypothesized that lysin B
112 provides a fitness advantage for optimal bacterial lysis and phage release since deletion of lysin
113 B results in viable phages with reduced plaque and burst size [27].
114 In phages that infect Gram-positive hosts the presence of genes that encode holin-like
115 proteins has primarily been characterized by bioinformatic analysis and many of the phages
116 contain more than one gene encoding a TMD protein that could serve as a holin or antiholin.
117 Currently there are reports on host lysis by phages that infect *Staphylococcus aureus* [35-37],
118 *Bacillus sp*. [38], *Lactococcal sp*. [39], *Oenococcus oeni* [40, 41], *Streptococcus sp* [42],
119 *Gordonia rubripertincta* [43-45] and *Mycobacterium sp*. [46-53]. The holin function for the

120 encoded TMD proteins in most of these reports is based primarily on the proximity of the TMD
121 gene/s near an endolysin. Where biochemical work is reported, the majority has been carried
122 out using exogenous expression of the TMD genes in *E. coli*. However, there are several
123 reports on phages that infect *Mycobacterium smegmatis* where gene deletion has been utilized
124 to evaluate lysis function of the predicted holin proteins.

125 The first study evaluated two genes encoding TMD proteins that are found directly
126 downstream of the *lysin A* and *lysin B* in the F1 cluster phage Ms6 [48-50]. Ms6 gene *26*
127 encodes an 88 amino acid protein with 2TMDs while gene *27* encodes a 124 amino acid protein
128 with 1TMD. Deletion of gene *26* resulted in reduced lysis timing, reduced plaque size but wild
129 type burst size, while deletion of gene *27* resulted in delayed lysis timing, increased plaque size
130 and increased burst size. However, there are limitations to these findings because holin function
131 was not verified using energy poisons and the mutant phages were not tested in liquid lysis
132 assays in the *M. smegmatis* host versus *E. coli*. In addition, the experiments to assess function
133 and interaction of the two proteins were carried out using recombinant *E. coli* expression
134 systems that are not physiologic. Thus, while it appears that both proteins are needed for the
135 lysis event, it is unclear how each is contributing to the lysis of the *M. smegmatis* host.

136 The second set of studies evaluated phage D29, a cluster A2 phage that also infects *M.*
137 *smegmatis* [51-54]. D29 has a lysis cassette with a *lysin A* (gene *10*), 2TMD holin (gene *11*) and
138 a *lysin B* (gene *12*). It is important to note that the 2TMD holin of D29 is not an ortholog to the
139 2TMD protein in Ms6 and differs significantly in amino acid sequence and size. The lysis
140 cassette that is also distinct from most other actinobacteriophages in that it has no other genes
141 encoding holin-like TMD proteins within or near the putative lysis cassette. Deletion of gene *11*
142 results in a viable phage with a different phenotype that the 2TMD deletion in Ms6 [51].
143 D29_Δ*11* phage shows a modest 30% reduced plaque size, slightly delayed lysis timing and
144 reduced burst size [51]. The lack of a more severe lysis phenotype is surprising given that gp11
145 is the only defined holin, especially since the D29 lysin A does not have a defined signal peptide

146 or SAR-like domain for export [31, 32]. However, it has been reported that the D29 lysin A may
147 be exported prior to lysis in a yet to be defined pathway that appears to be independent of the
148 holin [31, 32]. Alternatively, the modest lysis phenotype could also indicate that D29 has
149 additional holin-like genes that are not located within the defined “lysis cassette” region. Such a
150 scenario has recently been described in a bioinformatic study of the lysis cassettes of 77
151 phages that infect the Gram-positive *Gordonia rubripertincta* strain [44]. This study showed that
152 there was a high level of diversity of the lysis cassette gene organization and that putative holin-
153 like genes could be identified in genomic regions distal to the endolysin containing lysis
154 cassettes [44]. This study also showed that most of the phages evaluated had at least two holin-
155 like genes.

156 In summary, there is limited biochemical and genetic analysis of host lysis pathways by
157 phages that infect Gram-positive hosts, especially within the host bacteria. Consistent findings
158 suggest: 1) the putative holin genes do not appear to have dual start motifs like those identified
159 in lambda and phage 21; 2) that most annotated phages have multiple genes predicted to
160 encode holin-like TMD proteins; 3) that the TMD proteins are predicted to have 1, 2, or 4 TMDs;
161 and 4) that the putative holin-like genes can be bioinformatically identified outside of lysis
162 cassettes even in phages that have compact genomes of < 60,000bp. Of these findings, one of
163 the most intriguing is the presence of multiple genes that encode predicted holin-like TMD
164 proteins. Since antiholins have not been experimentally identified in phages that infect Gram-
165 positive hosts, one interpretation of these data are that holins and antiholins are expressed from
166 distinct genes as shown for *E. coli* phages P2 and T4 [16, 17, 55, 56]. It is also possible that
167 some of the TMD genes encode proteins with spanin-like functions that interact with the
168 complex cell wall of the Gram-positive bacteria. This hypothesis is supported by a report that
169 identified a 177 amino acid protein termed LysZ, that is encoded by phages that infect
170 *Corynebacterium glutamicum* and may function to disrupt the integrity of the bacterial cell wall
171 [57]. The current study aims to evaluate how two predicted holin-like TMD proteins encoded by

172 phages Girr and NormanBulbieJr (NBJ) function in the lysis pathway of *Mycobacterium*
173 *smegmatis* mc^2 155 by utilizing recombineered phages and multiple lysis assays under
174 physiological growth conditions. The findings show that both proteins termed, LysF1a and
175 LysF1b function as holins and are required for efficient bacterial lysis. The results also show that
176 the expression of the LysF1b protein is required for efficient functioning of the LysF1a protein
177 and that the LysF1a is not an antiholin. These results suggest a novel model for host lysis that
178 requires two holins with distinct membrane topologies.

179 **MATERIALS AND METHODS**

180 **Bioinformatic analysis of transmembrane domains and AlphaFold3 analysis**

181 The identification of transmembrane domains (TMD) and protein topologies was carried
182 out essentially as described by Pollenz et al., 2024 [44] utilizing Deep TMHMM (v1.0.24) [58,
183 TOPCONS (v2.0) [59], SignalP-5.0 and SignalP-6.0 [60], LipoP 1.0 [61] and HHpred
184 (databases: PDB_mmCIF70_30_Mar; Pfam-A_v37) [62]. All membrane proteins described in
185 this report had 100% consensus predictions of TMD domain location, number and protein
186 topology in all programs. Structural predictions of proteins and protein-protein interactions were
187 determined using AlphFold3 [63]. For single proteins, pTM scores >50% indicate high
188 confidence in the model predictions. For protein-protein interactions, ipTM scores <90% are
189 considered low confidence and should be used with caution [63]. All amino acid alignments
190 were performed using Clustal Omega [64].

191 **Bacterial strains, growth and plaque assay**

192 The list of bacterial strains, phage and plasmids utilized in this study is presented in
193 Table 1. *Mycobacterium smegmatis* mc^{2}155 [65] was used as wild type host for all phage
194 related experiments. *M. smegmatis* ∆mtpA and *M. smegmatis* ∆mtpA-comp are described in
195 [66]. *M. smegmatis* strains were propagated on Middlebrook 7H10 agar supplemented with 10%
196 Albumen Dextrose Complex (ADC; 5% albumen, 2% dextrose, 154mM NaCl) at 37°C. To

197 generate saturated stock cultures, a single colony of *M. smegmatis* was propagated in 25ml of

198 Middlebrook 7H9 media supplemented with 10% ADC, 1mM $CaCl_2$, 0.5% glycerol and 0.05%

199 Table 1. Bacterial Strains, Phage and Plasmids

Bacterial Strains	**Genotype/Features**	**Reference/Source**
M. smegmatis	*Mycobacterium smegmatis* mc^2 155	65
M. smegmatis ΔmptA	*Mycobacterium smegmatis* mc^2 155 lacking the mptA enzyme	66
M. smegmatis ΔmptA-comp	*ΔmptA* strain carrying complementing mtpA expression plasmid	66
E. coli	*Escherichia coli* NEB5α $F'I^Q$	New England Biolabs
Bacteriophage	**Genotype/Features**	**Source**
Phage Girr_WT	Mycobacteriophage Girr	68. PhagesDB: https://phagesdb.org/phages/Girr
Phage Girr_*Δ29*-20	Girr_WT with deletion of gene *29*	This study
Phage Girr_*Δ29*-25	Girr_WT with deletion of gene *29*	This study
Phage Girr_*ΔlysF1a*	Girr_WT with deletion of gene *34*	This study
Phage Girr_*ΔlysF1b*	Girr_WT with deletion of gene *35*	This study
Phage NBJ_WT	Mycobacteriophage NormanBulbieJr	69. PhagesDB: https://phagesdb.org/phages/NormanBulbieJr
Phage NBJ_*Δ29*	NBJ_WT with deletion of gene *29*	This study
Phage NBJ_*ΔlysF1a*	NBJ_WT with deletion of gene *33*	69
Phage NBJ_*ΔlysF1b*	NBJ_WT with deletion of gene *34*	This study
Plasmids	**Features**	**Source**
pExTra-Girr_*29*	pExTra01::(Ptet-Girr_*34*-mcherry); Kan^R	68
pExTra-Girr_*34*	pExTra01::(Ptet-Girr_*34*-mcherry); Kan^R	68
pExTra-Girr_*35*	pExTra01::(Ptet-Girr_*35*-mcherry); Kan^R	68
pExTra-NBJ_*29*	pExTra01::(Ptet-NBJ_*29*-mcherry); Kan^R	69
pExTra-NBJ_*32*	pExTra01::(Ptet-NBJ_*32*-mcherry); Kan^R	69
pExTra-NBJ_*33*	pExTra01::(Ptet-NBJ_*33*-mcherry); Kan^R	69

pExTra-Waterfoul_*32*	pExTra01::(Ptet-Waterfoul_*32*-mcherry); Kan^R	67
pExTra-Waterfoul_*32*ΔN	pExTra01::(Ptet-Waterfoul_*32(truncation of N-terminal TMD)*-mcherry); Kan^R	This study
pExTra-Waterfoul_*32*ΔC-40	pExTra0 ::(Ptet-Waterfoul_*32(truncation of C-terminal 40aa)*-mcherry); Kan^R	This study
pJV53	Acetamide inducible plasmid with Ched9c gene *60-61*. Kan^R	70

200

201 Tween-80 with shaking (225rpm) at 37°C. For all liquid lysis and one-step experiments, 100ul of
202 saturated stock was added to 250ml baffled flasks containing 55ml of supplemented 7H9
203 without Tween. Cultures were shaken (225rpm) overnight at 37°C and utilized in experiments
204 the next day while in log phase growth (OD_{600} <0.8). Titering experiments showed that an *M.*
205 *smegmatis* culture at an OD_{600} of 1.0 was equal to ~6.5 x 10^7 CFU/ml. This value was utilized
206 when phages were infected at different MOIs. Plaque assays were completed by mixing the
207 appropriate amount of phage with 250ul of saturated *M. smegmatis* in Middlebrook 7H9 media
208 supplemented with 10% ADC, 1mM $CaCl_2$ and 0.5% glycerol. The mixture was vortexed and
209 incubated at 22°C for 10 minutes. Following the infection, the sample was mixed with 4-5ml of
210 top agar (Middlebrook 7H9, 1mM $CaCl_2$, 0.5% agar) and plated immediately onto 7H10 agar
211 plates. Plates were allowed to harden and placed in a 37°C bacterial incubator for 16-48 hrs.
212 Competent *M. smegmatis* cells for recombineering or for plasmid transfection and
213 complementation studies were prepared as described previously [28, 67-69]. *Escherichia coli*
214 NEB5α $F'I^Q$ (New England Biolabs) was used for plasmid amplification and purification and
215 grown in LB broth or on LB agar supplemented with 50ug/ml kanamycin sulfate and.

216 **Plasmid constructs, *M. smegmatis* transformation and complementation analysis**

217 All PCR primers utilized in this study are shown in Table S1. To generate the inducible
218 expression plasmids pExTra_Waterfoul_*32ΔN*, pExTra_Waterfoul_*32ΔC40*,

219 pExTra_Waterfoul_32 was PCR amplified with Q5 DNA polymerase (New England Biolabs)
220 using Waterfoul specific primers containing with pExTra homology regions (Table S1). Purified
221 PCR products (were ligated into linearized pExTra01 using isothermal assembly (NEB HiFi 2x
222 Master Mix) as described [65-67]. Recombinant plasmids were recovered by transformation of
223 *E. coli* NEB5α F′I^Q and colonies selected on LB agar supplemented with 50μg/μl kanamycin
224 sulfate. Plasmid DNA was purified using the GeneJet kit (Fisher) and all plasmids were
225 sequence-verified by Sanger sequencing using the pExTra Seq primer (Azenta). For generating
226 complementing strains, competent *M. smegmatis* cells were prepared as described [67-69] and
227 40μl mixed with 100ng plasmid DNA in a 1mm electroporation cuvette. The sample was
228 electroporated with 1800V and the time constant set to 5.0 msec. Following electroporation, the
229 sample was mixed with 950μl of supplemented 7H9 media without Tween and shaken (225rpm)
230 at 37°C for 120 minutes. Following the recovery period, 10μl-100μl aliquots were spread on
231 7H10 agar plates supplemented with 10μg/μl kanamycin sulfate and incubated at 37°C for 3-5
232 days. To generate cultures for plaque assay, single colonies of *M. smegmatis* carrying the
233 appropriate plasmid were harvested into 25ml of supplemented 7H9 media containing 10μg/μl
234 kanamycin sulfate. Cultures were shaken (225rpm) at 37°C for 24-48 hours. Saturated cultures
235 at OD_{600} > 1.5 were centrifuged at 6200rpm for 10 minutes and the pellets resuspended in
236 supplemented 7H9 media (without Tween) to a final OD_{600} of 2.0. These cells were utilized for
237 phage infection and then mixed with 4.5ml top agar supplemented with 10ng/μl kanamycin
238 sulfate with or without 100ng/μl anhydrotetracycline (aTc). The mixture was added to 7H10 agar
239 containing 10μg/μl kanamycin sulfate supplemented with or without 100ng/μl aTc and incubated
240 at 37°C for the times indicated in the results section.

241 **Bacteriophage recombineering and genome sequencing**

242 All gblocks and PCR primers utilized in this study are shown in Table S1. The deletion of
243 genes in phage Girr and NBJ were carried out using the Bacteriophage Recombineering of

244 Electroporated DNA (BRED) procedure as described [28, 70], with the following modifications.
245 Phage genomic DNA was purified using the Wizard DNA Clean up kit (Promega). dsDNA
246 recombineering substrates were synthesized as gblocks (Integrated DNA Technologies). To
247 generate µg quantities of dsDNA substrates, gblocks were solubilized in water to 10ng/µl and
248 PCR amplified with gblock specific primers using 2X Q5 master mix (New England Biolabs).
249 PCR products were purified using Zymoclean DNA recovery (Zymoresearch). To generate
250 recombinant phage, 200-400ng dsDNA substrate was mixed with 100ng phage genomic DNA
251 and incubated on ice for 10min. The DNA mixture was added to 100µl of recombineering *M.*
252 *smegmatis* in a 2mm electroporation cuvette and electroporated at 2500V with the time constant
253 set to 20.0 msec. Following electroporation, 900µl of supplemented 7H9 media was added to
254 the cells and they were shaken (225rpm) at 37°C for 90 minutes. Following the recovery period,
255 the sample was mixed with 250µl of saturated *M. smegmatis* and plated with 5ml 7H9 top agar
256 onto 7H10 agar plates. Plates were incubated at 37°C for 18-24 hours to recover primary
257 plaques. Primary plaques were picked into 120µl of phage buffer (10 mM Tris-HCl, pH 7.5; 10
258 mM $MgSO_4$, 68.5 mM NaCl; 1mM $CaCl_2$), vortexed, and incubated at 22°C for 2-8 hrs. The
259 presence of mutant phage genomes was determined by Deletion Amplification Detection Assay
260 (DADA) PCR [28] using a 20µl reaction with: 1µl of plaque sample, 2µl of 0.2 µM DADA primer
261 mix (1:1 mix of For and Rev primers), 5µl glycerol (40%), 2µl water and 10µl OneTaq 2x Master
262 Mix (New England Biolabs). PCR conditions were: 94°C for 1 minute followed by 35 cycles of
263 94°C-1min/66°C 1min and a final 66°C step for 5 minutes. Positive primary plaque samples
264 were serially diluted and plated on wild type or complementing *M. smegmatis* as indicated.
265 Secondary plaques were picked as above and screened by standard PCR using gene specific
266 flanking primers. Pure populations of mutant phage were evaluated by full genome sequencing
267 as described [71, 72]. Briefly, Genomic DNA was used to create sequencing libraries with the
268 NEB XLEP-P1 kit. Sequencing was performed by the Pittsburgh Bacteriophage Institute and the
269 library run on an Illumina NextSeq 1000 instrument. Raw reads were trimmed with cutadapt 4.7

270 (using the option: –nextseq-trim 30) and filtered with skewer 0.2.2 (using the options: -q 20 -Q
271 30 -n -l 50) prior to assembly. The resulting sequences were assembled using Consed (v29.0)
272 with Unicycler (v5.0) and contigs checked for completeness, accuracy, and genome termini.
273 Final phage contigs were aligned to wild type phage to identify deletions and point mutations.

274 **Plaque size analysis**

275 Plaques were generated using the plaque assay procedure described above. For
276 experiments where plaque size would be evaluated between several different phages, identical
277 bacterial samples, incubation times, phage concentrations and top agar amounts were utilized.
278 Plaque size was evaluated using ImageJ software [73] and by manual measurement using
279 photos embedded in PowerPoint and custom rulers. In most experiments, results are presented
280 for an average of 50 plaques and the statistical significance of measurements determined by
281 unpaired t-test (https://www.graphpad.com/quickcalcs/ttest1/). Plaque volume was calculated by
282 the formula $\pi r^2 h$ where r is the radius of the plaque and h was set to 1mm for the top agar
283 thickness.

284 **Liquid lysis assay**

285 Liquid lysis assays were carried out essentially as described by Payne et al., 2009 [27]
286 with the following modifications. Briefly, overnight cultures of *M. smegmatis* in log phase growth
287 were diluted to an OD_{600} of 0.25-0.30 in supplemented 7H9 without Tween and 40ml of culture
288 was added to 250ml baffled flasks. High titer phage lysate was added to the cultures to create
289 an MOI of 10 and the mixture set at 37°C for 30 minutes without shaking. T_0 for all experiments
290 was the time of phage addition. After 30 minutes (T_{30}), the cultures were constantly shaken a
291 225rpm and aliquots of cells removed with a syringe and sterile needle from the shaking culture
292 without stopping the incubator. The OD_{600} of the sample was immediately recorded for each
293 aliquot using a GENESYS spectrophotometer (Fisher Scientific). In some experiments, KCN
294 (1M in water), or $CHCl_3$ (100%) was added directly to the shaking culture to produce a final

295 concentration of 10mM or 1%, respectively. All liquid lysis experiments were repeated at least
296 five separate times and representative experiments are presented.

297 **ATP assay**

298 The presence of ATP in culture supernatants was determined utilizing the ENLIGHTEN
299 kit (Promega). Briefly, liquid lysis assays were carried out as described above. A 500ul aliquot of
300 culture was removed at indicated time points and immediately passed through a 0.2μ syringe
301 filter to remove bacteria. The sample was frozen at -20°C prior to analysis. The presence of ATP
302 in culture supernatants was determined by mixing 5μl with 50μl ENLIGHTEN reagent
303 (Promega), mixing for 5 seconds and then reading the integrated luminescence over 10
304 seconds using a GloMax luminometer (Promega). To assure that the readings were within the
305 linear range of the instrument an ATP standard curve was utilized.

306 **One-step growth curves and burst size determination**

307 Several experimental procedures have been utilized for one-step growth curves with
308 Gram-positive bacteria [32, 47, 49, 51]. In our hands, none of these procedures generated
309 consistent results or provided the ability to directly measure burst size. Thus, we developed a
310 one-step protocol that is illustrated in Figure S1 and described below. To prepare the cells, the
311 OD_{600} of fresh overnight cultures of *M. smegmatis* in log growth were determined and 10ml
312 centrifuged at 3,000rpm for 10 minutes. The cells were resuspended in supplemented 7H9 to a
313 final concentration equal to an OD_{600} of 3.2/ml. 250μl of cells (~5 x 10^7 cfu) were added to
314 microfuge tubes and ~5 x 10^7 phage added to the cells to create an MOI of 1. The same amount
315 of phage were also added to 250μl of supplemented 7H9 media without cells to verify the titer
316 and determine the level of phage adsorption. The mixture was vortexed and set at 37°C for 30
317 minutes without shaking. T_0 for all experiments was the time of phage addition to the cells. After
318 30 minutes, 750μl of supplemented 7H9 was added to all samples. Samples were vortexed and
319 centrifuged at 6,200rpm for 4 minutes to separate unabsorbed phage. The supernatant was
320 saved for analysis of titer and adsorption, and the cell pellet immediately resuspended in 1ml

321 supplemented 7H9, vortexed and diluted 1:10,000 into 70ml of supplemented 7H9 in baffled
322 250ml flasks. An aliquot was removed and 5μl, 12.5μl and 25μl used for plaque assay to
323 determine the number of infectious centers to determine the precise number of infected cells. A
324 second aliquot was removed and filtered through a 0.2μ syringe filter and 150μl utilized for
325 plaque assay to test for unabsorbed (free) phage at T_{45} minutes (the first one-step data point).
326 The flask was placed in a 37°C incubator and constantly shaken at 225rpm for the duration of
327 the experiment. At specified time points, 500μl aliquots were removed from the shaking flasks
328 and each sample immediately passed through a 0.2μ syringe filter to remove cells and collect
329 free phage. The amount of phage in each sample was determined by performing plaque assays
330 using 150μl of serially diluted samples (usually 10^0 to 10^{-4} dilutions were sufficient). The phage
331 titer in the flask, expressed as PFU/ml was determined at each time point by counting the
332 plaques on each plate, dividing by the volume of phage used in the infection (150μl), multiplying
333 by the dilution factor and then multiplying by 10^3. The number of infectious centers in the
334 infected 70ml culture was determined by counting the plaques, dividing by the volume used for
335 the plaque assay and multiplying by 70,000. The original phage titer and the percentage of
336 adsorbed phage was determined by spot titers and plaque assay of the serially diluted
337 supernatants collected from the samples of phage with and without the added cells. Since the
338 number of cells and phage used in these experiments was held constant, this procedure
339 consistently produced ~3.5-5.5 x 10^7 infectious centers. This procedure also resulted in
340 essentially zero unabsorbed phage in the culture at the start of the one-step assay. Burst size at
341 all time points could be directly determined by dividing the total phage in the 70ml culture by the
342 number of infectious centers. All phages were evaluated through a minimum of three separate
343 assays. A representative data set showing the raw data for adsorption, infections centers and a
344 one-step assay is provided in Figures S2 and S3.
345
346

347 **RESULTS AND DISCUSSION**

348 **Topologies of Holin-like TMD Proteins Within the Lysis Cassettes of F1 Cluster Phages**
349 **Girr and NormaBulbieJr.**

350 To investigate the contribution of predicted holin-like proteins in the lysis of *M.*
351 *smegmatis*, it was desirable to begin work in phages that had a defined lysis cassette and prior
352 wet-lab data. F1 cluster phages Girr and NormanBulbieJr (NBJ) were selected since both
353 phages have a define lysis cassette and a full genome cytotoxicity screen has been reported for
354 both phages [68, 69]. Girr and NBJ have an average nucleotide identity of 89.86% but only
355 share 69 of 102 genes. Both phages have a defined lysis cassette organization located
356 downstream of the *tape measure* and *minor tail* genes and encode a Lysin A enzyme predicted
357 to target the peptidoglycan layer and a Lysin B that targets the linkage of the arabinogalactins to
358 the mycolic acids. The *lysin B* gene is directly followed by two genes encoding proteins that
359 have predicted TMDs (Girr *34* and *35* and NBJ *32* and *33*).

360 It was first important to bioinformatically evaluate the predicted topologies of these TMD
361 proteins and determine how they compared to previously characterized holins or other phage
362 proteins involved in bacterial lysis. Girr *34* and NBJ *32* encode small 80aa and 77aa proteins,
363 respectively, that have two predicted TMD regions and an N-in-C-in topology by all TMD
364 prediction programs (Figure 2A). The proteins are 97% identical and have cytoplasmic N and C-
365 terminal domains that each contain four charged amino acids. The presence of two TMDs and
366 the N-in-C-in topology is like the phage 21 S^{21} type II pinholin (Figure 2BC). However, the
367 presence of a pinholin is typically associated with a SAR-endolysin that is secreted to the
368 periplasmic space prior to lysis triggering [10, 11, 13]. Analysis of the Girr or NBJ Lysin A
369 proteins by the various TMD prediction programs and AlpahFold3, show no evidence of SAR
370 domains or signal sequences (Figures S4-S6), and this is consistent with previous analysis of
371 Lysin A proteins from phages that infect *M. smegmatis* [20]. Thus, it is critical to contrast several
372 structural differences of gp32 and gp34 to the canonical $S^{21}68$ pinholin and $S^{21}71$ antiholin.

373 First, the $S^{21}68$ holin protein has only 3 N-terminal amino acids prior to the TMD1 and
374 this feature is a critical to its function as a holin and allows the TMD1 to become cytoplasmic
375 (Figure 2BC) [11-15]. Second, the S^{21} gene has a dual start motif that produces both the $S^{21}68$
376 holin protein and the $S^{21}71$ antiholin after phage infection [11-15]. The difference in the two
377 proteins is the addition of the extra basic K residue to the N-terminal cytoplasmic domain of
378 $S^{21}71$ that limits the TMD1 from exiting the membrane to the same degree as the $S^{21}68$ holin
379 (Figure 2BC; [11-15]). Thus, the expression of $S^{21}71$ keeps a percentage of the $S^{21}68$ in an
380 inactive dimer until triggering at which time the $S^{21}71$ converts to an active holin [13-15, 74, 75].
381 Third, the $S^{21}68_{IRS}$ protein is an engineered version of $S^{21}68$ that adds the MRYIRS motif and 4
382 charged residues in the N-terminal cytoplasmic domain that creates a dominant negative
383 version of the antiholin that is poorly triggered to an active holin [74]. Neither Girr gene *34* nor
384 NBJ gene *32* have a dual start motif that generates multiple products of the same open reading
385 frame. Genes *34* and *32* encode a single protein product that has a predicted N-terminal
386 cytoplasmic domain of 13-16 amino acids of which four are charged and two others are polar.
387 Therefore, the N-terminal topology and the number of charged amino acids in Girr gp34 and
388 NBJ gp32 are more similar with the $S^{21}71$ antiholin and $S^{21}68_{IRS}$ and would predict that TMD1 of
389 these proteins remains embedded in the membrane. In addition, the TMDs of S^{21} both contain
390 GxxxG motifs that are predicted to contribute to homotypic and/or heterotypic helix interactions
391 of the monomers that facilitate the formation of the pinholes [74, 75]. While TMD1 and TMD2 of
392 Girr and NBJ have a high percentage of GA residues (Figure 2A), they lack defined GxxxG
393 domains found in S^{21}. Finally, Girr gp34 can't be modeled with high confidence by AlphaFold3
394 into either a monomer or a heptamer (Figure S7). Taken together, this data suggests that Girr
395 gp34 or NBJ gp32 are unlikely to function as a type II holin. Based on the literature we will
396 designate these proteins as LysF1a due to a predicted function in lysis (lys) and being first
397 identified in F1 cluster phages.

398 Since there is a second gene encoding a protein with a single TMD directly downstream
399 of the *lysF1a* gene, we hypothesized that this protein may also be involved in the lysis pathway.
400 Girr *35* and NBJ *33* both have -4bp ATGA overlaps to the upstream *lysF1a* gene and encode
401 98% identical 124aa proteins with a single N-terminal TMD and a predicted N-out-C-in topology
402 by all TMD prediction programs (Figure 3A). Both proteins have a 22 amino acid extracellular
403 domain followed by the single TMD. There are four basic residues following the TMD and
404 AlphaFold3 predicts an extended helical cytoplasmic C-terminal domain that contains ~50%
405 KRDE charged residues typical of holins [10, 11]. Figure 3B shows the AlphaFold3 models and
406 predicted topologies of representative proteins that have a single TMD and have been shown to
407 be involved in the bacterial lysis pathway for comparison gp33 and gp35. Most pertinent is the
408 type III holin typified by the T protein of phage T4 that forms large 1um holes like canonical type
409 I holins [16, 17]. However, the type III holin has <20% amino acid identity to gp33 and gp35, is
410 much larger at 221 amino acids and has the opposite membrane topology with a globular
411 extracellular domain critical to its holin function (Figure 3B). It noteworthy that spanins also have
412 a single TMD and model with an extended helical prediction, but like the type III holins, these
413 proteins are also oriented in a N-in-C-out topology that has been shown experimentally and is
414 also predicted by the TMD prediction programs (Figure 3B; [10, 11]). Interestingly, there is a
415 recent report regarding phages that infect the Gram-positive *Corynebacterium glutamicum*
416 strain. The authors have characterized a protein with 1 TMD that is termed LysZ and is
417 proposed to interact with lipid-anchored glycans on the extracellular side of the IM to promote
418 efficient lysis [57]. However, like the type III holin, LysZ is much larger than the Girr and NBJ
419 proteins and it is proposed to have a N-in-C-out topology that allows it to interact with the lipid-
420 anchored glycans [57]. Thus, Girr gp35 and NBJ gp33 are most similar in structure and
421 membrane topology to the recently identified phage Mu releasin protein (Figure 3B) [18].
422 Releasin however, is named due to its function to release the Mu SAR-endolysin from the
423 membrane in a holin independent manner [18]. Mu also has <20% amino acid identity to gp33

424 and gp35 and does not possess the highly charged cytoplasmic domain. Thus, of all the
425 characterized proteins involved in lysis that have 1 TMD, gp35 and gp33 appear to represent a
426 novel class of proteins and will be termed LysF1b since the gene is downstream of the *lysF1a*.

427 **Deletion of Individual *lysF1a* and *lysF1b* Genes in Phage Girr are Viable While Deletion of**
428 **Both is Lethal**

429 To evaluate the function of the *lysF1a* and *lysF1b* genes, the BRED recombineering
430 method was utilized to delete them in both Girr and NBJ as described in Methods. Several
431 primary plaques were positive for each deletion and pure populations of Girr_*ΔlysF1a*,
432 Girr_*ΔlysF1b*, NBJ_*ΔlysF1a*, and NBJ_*ΔlysF1b* were recovered from secondary plaques. Figure
433 4 shows the lysis cassette organizations of the Girr mutants and the PCR verification of the
434 gene deletions from clonal high titer lysates. The data for NBJ is shown in Figure S8 and
435 deletion of gene *33* is also presented in Wise et al. [69]. The genome structure of all deletions
436 was confirmed by sequencing the immediate region of the deletion and by whole genome
437 sequencing to validate that there were no point mutations outside of the targeted gene deletion
438 region. Since deletion of either of the individual TMD genes resulted in viable phage, it was of
439 interest to test whether a double deletion of both TMD genes was viable. For these studies
440 Girr_*ΔlysF1a* DNA was utilized to delete *lysF1b* and a positive primary plaque was picked,
441 resuspended in buffer and plated to recover ~250-1000 isolated plaques on complementing and
442 non-complementing *M. smegmatis* as shown in the protocol schematic in Figure 5A. Since
443 BRED was being used, positive primary plaques will have a mixture of the phage used for
444 recombineering and the mutant. Lysates representing all the phage from secondary plaques
445 were recovered and evaluated by DADA PCR to test for the presence of the double mutant.
446 Figure 5B shows that the double mutant genotype is not recovered on wild type *M. smegmatis*,
447 even when 800PFU were plated (gel lanes 3-6). However, when >250 phage particles are
448 plated on the complementing *M. smegmatis* strain transfected with pExTra-Girr*34* expressing

449 LysF1a, a positive DADA band is observed (Figure 5B, gel lane 8). The inability to recover a
450 phage with the deletion of both *lysF1a* and *lysF1b* is highly supportive that the expression of
451 both Girr LysF1a and LysF1b are required for Girr viability. A lethal phenotype is observed when
452 holin genes are deleted in *E coli.* phages that encode canonical holins required for endolysin
453 release [10, 11].

454 **Deletion of Individual *lysF1a* and *lysF1b* Genes in F1 Phages Result in Reduced Plaque**
455 **Size**

456 To assess the phenotypes of the mutant phage, equal concentrations of Girr_WT,
457 Girr_*ΔlysF1a* and Girr_*ΔlysF1b* were used to infect *M. smegmatis* and the total number of
458 recovered plaques and plaque sizes evaluated. All phages formed plaques with equivalent
459 efficiencies under the standard assay conditions described in Methods suggesting no defects in
460 adsorption (Figure S9). However, both Girr_*ΔlysF1a* and Girr_*ΔlysF1b* presented with
461 significantly smaller plaques than Girr_WT (Figure 6) as did NBJ_*ΔlysF1a* and NBJr_*ΔlysF1a*
462 (Figure S10). A summary of the plaque size data for both Girr and NBJ is presented in Table 2.
463 Deletion of the *lysF1a* gene from Girr or NBJ results in ~40% reduction in plaque diameter and

464 **Table 2 Plaque sizes in WT Girr and *lysF1a* and *lysF1b* deletion mutants.**

PHAGE	Plaque size (mm)	% of WT (diam.)	Plaque (vol, mm^3)	% of WT (plaque vol)
NBJ_WT	3.49 +/- 0.533	100	11.479	100
NBJ_Δ*lysF1b*	1.23 +/- 0.225*	35.24*	1.425*	12.42*
NBJ_Δ*lysF1a*	2.05 +/- 0.660*	58.73*	3.96*	34.50*
Girr_WT	3.88 +/- 0.731	100	14.188	100
Girr_Δ*lysF1b*	1.28 +/- 0.376*	32.98*	1.544*	10.88*
Girr_Δ*lysF1a*	2.31 +/- 0.719*	59.53*	5.029*	35.44*

465

466 *M. smegmatis* was infected with identical numbers of phage and plaque size determined after
467 36 hrs. of growth at 37°C. Plaque diameter was measured using ImageJ. Data is presented as
468 average +/- standard deviation for a minimum of 50 individual plaques. * = statistically significant
469 from Girr or NBJ WT phage *p<0.0001.*
470

471 a 65% reduction in plaque volume, while deletion of the *lysF1b* is more severe showing a ~65%
472 reduction in plaque diameter and near 90% reduction in plaque volume. To validate that these
473 plaque size reductions were directly related to the loss of *lysF1a* or *lysF1b* genes, *M. smegmatis*
474 containing complementing expression plasmids were infected with the mutant phages and
475 plaque size evaluated as described in Methods. Since both Girr LysF1b and NBJ LysF1b are
476 highly toxic when exogenously expressed in *M. smegmatis* [68, 69], complementation of the
477 *lysF1b* deletions first utilized Waterfoul gp32. Waterfoul is a K5 cluster phage with a canonical
478 lysis cassette and gene *32* encodes a 1TMD with the same general size and membrane
479 topology as Girr LysF1b (Figure 3C) and is not toxic when induced by aTc in *M. smegmatis* [67].
480 When M*. smegmatis* transfected with Waterfoul gp32 is infected with Girr_*ΔlysF1b* in the
481 presence of aTc, there is a significant increase in plaque size compared to untreated cells
482 (Figure 6A). Importantly, the increase in plaque size was not observed when the N-terminal
483 TMD domain or the highly charged C-terminal 40 amino acids of Waterfoul gp32 were truncated
484 (Figure 6A). Thus, the complementation by Waterfoul gp32 requires the full-length protein.
485 Recently it has been reported that the pTet promoter in pExtra is leaky and that it is possible to
486 complete complementation analysis in the absence of aTc [68]. Thus, *M. smegmatis* was
487 transfected with pExTra-Girr*35* and pExTra-NBJ*33* and the resulting cells infected with
488 Girr_Δ*lys1b* as described in Methods. Figure 6B shows that there is a significant increase in
489 plaque size when Girr_Δ*lys1b* is plated on the complementing strains expressing the LysF1b
490 proteins compared to cells with the base pExTra01 vector. These results support that the
491 reduced plaque size of Girr_*ΔlysF1b* is directly attributable to the loss of *lysF1b.* Similarly, the
492 wild type plaque size is restored when *M. smegmatis* harboring the pExTra-Girr_*34* plasmid is
493 infected with Girr_*ΔlysF1a* (Figure 8). Thus, the loss of either *lysF1* gene appears to create a
494 lysis defect phenotype that is like the phenotype when the *lysin B* is deleted in phage Giles and
495 the cell wall components remain a barrier to efficient phage release [27].

496 **Deletion of Individual *lysF1* Genes Result in Distinct *M. smegmatis* Liquid Lysis**
497 **Phenotypes and ATP Release.**
498 A main function of holins is the control of the lysis timing by the destruction of the proton
499 motive force (PMF) [10, 11]. To assess lysis timing of Girr, NBJ and the *lysF1* mutants, liquid
500 lysis assays were performed where the optical density (OD_{600}) of infected log growth *M.*
501 *smegmatis* cultures is measured over time. Importantly, in all studies, once phage had been
502 allowed to absorb for 30 minutes, cultures were continually shaken even while samples were
503 withdrawn so that lysis would not be prematurely triggered by changing the culture conditions
504 [11, 76]. The data show that cultures infected with Girr_WT grow steadily until ~110 minutes
505 post infection. Beginning at 110 minutes, there is a significant drop in the OD_{600} of the culture
506 (triggering event) until it reaches a baseline of OD_{600} 0.10 at about 200 minutes (Figure 9A). In
507 contrast, Girr_*ΔlysF1a* grows until ~130 minutes and then shows a reduction in OD_{600} until 300
508 minutes that does not reach the same OD_{600} baseline as Girr_WT even after 480 minutes of
509 incubation (Figure 9A). Strikingly, cultures infected with Girr_*ΔlysF1b* do not show a drop in
510 OD_{600} but appear to cease growing after ~200 minutes with only a slight decrease in OD_{600} over
511 the remaining growth period out to 480 minutes (Figure 9A). For NBJ_WT, OD_{600} begins to drop
512 after 130 minutes and like Girr_WT reaches a baseline of around OD_{600} 0.10 (Figure 9B).
513 NBJ_*ΔlysF1a* shows a delay in lysis timing like Girr_*ΔlysF1a*, but the delay is more pronounced
514 as the OD_{600} does not begin to drop until ~180 minutes post infection (Figure 9B). Just like
515 Girr_*ΔlysF1b*, NBJ_*ΔlysF1b* ceases to grow after ~200 minutes and does not show a significant
516 reduction in OD_{600} even after 480 minutes of growth (Figure 9B). Thus, in both phages, deletion
517 of *lysF1a* results in a triggering delay while deletion of *lysF1b* results in no defined triggering
518 event in this assay. It is interesting that Girr_WT and NBJ_WT show a ~20-minute difference in
519 triggering time and that a difference is also observed between Girr_*ΔlysF1a* and NBJ_*ΔlysF1a.*
520 These results may be due to differences in how the lysis cassette genes are expressed since

521 Girr has an HNH endonuclease gene between the *lysin A* and *lysin B* (Figure 1) and the
522 intergenic region between the *lysin B* gene and the *lysF1a* is 8bp in NBJ but 38bp in Girr (Figure
523 S11).

524 ATP release has been used as a measure of cell viability and membrane integrity
525 following phage infection [27, 51]. Figure 9C shows the ATP release from the same experiment
526 that is presented in Figure 9AB. As expected, ATP release for Girr_WT, NBJ_WT, Girr_*ΔlysF1a*
527 and NBJ_*ΔlysF1a* generally mirrors the time at which lysis is triggered and the culture OD_{600}
528 begin to decline. ATP levels in the media also peak when the OD_{600} baseline is reached at about
529 300 minutes (Figure 9C). In contrast, there is delayed but gradual increase in the amount of
530 ATP released from the cultures infected with Girr_*ΔlysF1b* and NBJ_*ΔlysF1b* out to 300
531 minutes. Although the ATP level does not reach that of Girr_WT or NBJ_WT, the release of ATP
532 confirms that cell integrity has been comprised after infection with the *lysF1b* mutants.
533 Collectively, the important finding from this data set is that an F1 phage with only the 1TMD
534 LysF1b protein can trigger the lysis event in the absence of the 2TMD lysF1a protein, but that
535 the lysF1a protein does not support significant bacterial lysis as measured by a drop in OD_{600}. In
536 fact, the liquid lysis results for Girr_*ΔlysF1b* and NBJ_*ΔlysF1b* are like those observed for the
537 lethal *lysin A* deletion in phage Giles where the cultures stopped growing and the OD_{600}
538 plateaued but did not decline [27]. The similarity in these results suggest that the lysis defects in
539 the *ΔlysF1b* phage may be related to the inability of the endolysins to efficiently cleave the cell
540 wall components because they are either not efficiently released from the infected cell or cannot
541 be activated in some manner.

542 **Energy Poisons Cause Early Triggering of F 1Cluster Phages with Deletion of the *lysF1a***
543 **Gene but not the *lysF1b* Gene in Liquid Lysis Assays**

544 The results presented so far indicate that the expression of both TMD proteins are
545 required for phage viability, but phages that express only the LysF1b protein can support

546 bacterial lysis while phages that express only LysF1a are viable but severely lysis
547 compromised. The diagnostic assay for holin function is the ability to cause early triggering of an
548 infected culture by the addition of energy poisons (e.g., cyanide or the protonophore
549 dinitrophenol) due to the disruption of the proton motive force (PMF) [11, 76]. This type of assay
550 has been utilized in nearly all the pioneering work on holin function of phages that infect *E. coli.*
551 [10, 11, 18]. *M. smegmatis* was infected with Girr_WT or Girr_*ΔlysF1a* and the OD_{600} of the
552 culture measured as described in Methods. At 110 minutes after infection, KCN (final
553 concentration of 10mM) was added directly to one culture of Girr_*ΔlysF1a* and to a culture of
554 uninfected cells. Figure 10A shows that Girr_WT triggers at ~110 minutes while Girr_*ΔlysF1a*
555 triggers at 130 minutes just as in Figure 9A. However, when KCN is added to a culture infected
556 with Girr_*ΔlysF1a*, there is a drop in OD_{600} beginning at ~120 minutes that clearly precedes the
557 drop in the untreated Girr_*ΔlysF1a* culture. KCN addition to uninfected cells results in immediate
558 cessation of growth, but not a significant drop in OD_{600}. To validate these results, studies were
559 repeated with the NBJ mutants. NBJ_WT triggers later than Girr_WT at ~130 minutes and
560 declines to OD_{600} 0.10 by 300 minutes as expected (Figure 10B). NBJ_*ΔlysF1a* shows delayed
561 triggering just as in Figure 9B and addition of KCN to a culture infected with NBJ_*ΔlysF1a* at
562 120 minutes results in lysis triggering by 130 minutes with a gradual reduction in OD_{600} that
563 mirrors the NBJ_WT. The ability of Girr_*ΔlysF1a* and NBJ_*ΔlysF1a* to trigger lysis, identifies the
564 1TMD LysF1b protein as a putative holin and not a releasin, since energy poisons do not trigger
565 lysis prematurely in phage Mu [18].
566 The next set of studies focused on the phages with deletion of the 1TMD *lysF1b* genes
567 to determine if they could also be triggered by the addition of KCN. Figure 10C shows the
568 results for Girr_*ΔlysF1b*. As previously shown in Figure 9A, *M. smegmatis* infected with
569 Girr_*ΔlysF1b* does not exhibit a defined triggering event as the cells simply cease growing with
570 a slight reduction in OD_{600} out to 480 minutes. Addition of KCN to the Girr_*ΔlysF1b* culture at

571 180 minutes results in a modest 30% reduction of OD_{600} between 180-240 minutes compared to
572 the Girr_*ΔlysF1b* untreated culture. However, following this initial decline, the level of change in
573 OD_{600} generally mirrors that of the untreated Girr_*ΔlysF1b* culture and the KCN treated *M.*
574 *smegmatis* control. In contrast, addition of 1% $CHCl_3$ to the Girr_*ΔlysF1b* culture at 180 minutes,
575 results in an immediate precipitous drop in OD_{600} to the level of Girr_WT indicating that the
576 endolysin enzymes are present and active in the cells. The results for NBL_*ΔlysF1b* are shown
577 in Figure 10D and exhibit near identical results to Girr_*ΔlysF1b* in that addition of KCN cause a
578 modest drop during the first hour after addition, and then an OD_{600} decline that mirrors the
579 untreated NBJ_Δ*lysF1b* culture and the KCN treated *M smegmatis*. Addition of $CHCl_3$ results in
580 the same type of sharp decline in OD_{600} to the level of the NBJ_WT baseline. Collectively, these
581 results show that phages expressing only the 2TMD LysF1a protein are not efficiently triggered
582 following disruption of the PMF but that the cells have the requisite enzymes for lysis since lysis
583 occurs immediately after addition of 1% $CHCl_3$. The inability of the LysF1a proteins to be
584 triggered by KCN is like the $S^{21}71$ or $S^{21}68_{IRS}$ antiholins [13, 74, 75].

585 **F1 Cluster Phage Deleted for *lysF1a* have Delayed Burst Timing While Phage Deleted for**
586 ***lysF1b* Deletion have Reduced Timing and Greatly Reduced Burst Size**

587 The previous results show that infection of *M. smegmatis* with either Girr_*ΔlysF1a* or
588 NBJ_*ΔlysF1a* results in a defined triggering (lysis) event that can be prematurely initiated by
589 addition of KCN. However, the results do not establish if phage have been efficiently released
590 from the lysed cells, the timing of the burst event and the burst size. Since it is not possible to
591 utilize lysogens to study phage release in *M. smegmatis*, one-step grow curves were utilized to
592 evaluate the various *lysF1a* and *lysF1b* mutant phages. The experimental set up for these
593 studies is fully described in the methods and representative raw data sets are also shown in
594 Figures S2 and S3. The one-step results from three different experiments utilizing Girr phages
595 are presented in Figure 11. Phage release from Girr_WT shows a lag time of ~180 minutes from

596 the time of infection and then a gradual phage release for 90 minutes before reaching a plateau
597 at ~300 minutes (Figure 11A). The slow release of phage over a 90-minute period is consistent
598 with the liquid lysis assays that showed an ~60-minute timeline of OD_{600} decline after triggering.
599 This is an important observation because there should not be a sharp, immediate lysis of all
600 cells and accompanying phage release since the phage infections are not synchronized but
601 carried out over a 30-minute period and the efficient release of phage from Gram-positive
602 bacteria may also be hampered by the extensive cell wall. Girr_*ΔlysF1a* shows a delayed lag
603 time by ~20 minutes compared to Girr_WT and a more prolonged period of phage release over
604 150 minutes before reaching a plateau. The overall burst size for Girr_WT over three
605 experiments was 277 +/- 81 PFU/cell. Girr_*ΔlysF1a* showed a lower burst of 255 +/- 75 PFU/cell
606 but this was not statistically different from the for Girr_WT. In contrast, Girr_*ΔlysF1b* shows a
607 very small but defined burst at ~ 210 minutes that is best illustrated when the data is plotted
608 independent of the other phages (Figure 11B). The overall burst size for Girr_*ΔlysF1b* is only
609 ~29.2 +/- 36 PFU/cell suggesting very poor efficiency of phage release from the infected cells.
610 Overall, this data is consistent with the plaque size and liquid lysis results and supports the
611 hypothesis that *M. smegmatis* integrity is compromised when infected with Girr_*ΔlysF1b* but the
612 release of phage progeny is severely impacted. In addition, the near wild type burst size
613 observed in cells infected with Girr_*ΔlysF1a*, further support the holin function of the LysF1b
614 protein.

615 **Lysis Recovery Mutants Isolated from Girr_*ΔlysF1b* or NBJ_*ΔlysF1b* Show Wild Type**
616 **Plaque Size and have Point Mutations in the *lysF1a* Gene**

617 Since both Girr_*ΔlysF1b* and NBJ_*ΔlysF1b* show significant plaque size defects it was
618 possible to screen for lysis recovery mutants (LRM) by assessing changes to the small plaque
619 size following multiple rounds of infection and replication. Figure 12A shows the presence of a
620 large plaque in a Girr_*ΔlysF1b* plaque assay after the second round of harvest and infection.

621 **Table 3. Lysis Recovery Mutants (LRM) from Δ*lysF1b* Phages.**

Phage	Type of mutation	Genetic location	Mutation Result
Girr_Δ*lysF1b*-LRM1	point mutation-nucleotide substitution	gene *35 (lysF1a)*	G66D
Girr_Δ*lysF1b*-LRM2	point mutation-nucleotide substitution	gene *35 (lysF1a)*	R19H
Girr_Δ*lysF1b*-LRM6	point mutation-nucleotide deletion	gene *35 (lysF1a)*	missense coding after A63 and premature stop at aa74: A63APRQPRNGFGD.STOP
Girr_Δ*lysF1b*-LRM7	point mutation-nucleotide substitution	gene *35 (lysF1a)*	G66D
Girr_Δ*lysF1b*-LRM8	point mutation-nucleotide insertion	gene *35 (lysF1a)*	stop after G66
Girr_Δ*lysF1b*-LRM11	point mutation-nucleotide insertion	gene *35 (lysF1a)*	stop after G66
Girr_Δ*lysF1b*-LRM12	point mutation-nucleotide insertion	gene *35 (lysF1a)*	stop after G66
Girr_Δ*lysF1b*-LRM14	point mutation-nucleotide substitution	gene *35 (lysF1a)*	G66D
Girr_Δ*lysF1b*-LRM15	point mutation-nucleotide insertion	gene *35 (lysF1a)*	stop after G66
Girr_Δ*lysF1b*-LRM16	point mutation-nucleotide substitution	gene *35 (lysF1a)*	A31T
NBJ_Δ*lysF1b*-LRM1	point mutation-nucleotide substitution	gene *33* (*lysF1a*)	A68E
NBJ_Δ*lysF1b*-LRM2	point mutation-nucleotide substitution	gene *33* (*lysF1a*)	A68E
NBJ_Δ*lysF1b*-LRM3	point mutation-nucleotide substitution	gene *33* (*lysF1a*)	A68E
NBJ_Δ*lysF1b*-LRM7	point mutation-nucleotide substitution	gene *33* (*lysF1a*)	D9A

622

623 When phages were recovered from the large plaque, serial diluted and replated, the wild type
624 plaque size was recovered across the full phage population (Figure 12B). This type of
625 experiment was repeated multiple times with Girr_Δ*lysF1b* and NBJ_Δ*lysF1b* and ten
626 independent Girr_Δ*lysF1b*-LRMs and four independent NBJ_Δ*lysF1b*-LRMs were recovered. All
627 Girr LRM mutants showed a large plaque phenotype compared to the parent Girr_Δ*lysF1b*

628 (Figure S11 and RSP, data not shown) and PCR analysis of the *lysF1a-lysF1b* genomic region
629 confirmed that all the LRM mutants contained the expected Δ*lysF1b* deletion (Figure S12). To
630 determine the location of any nucleotide mutations within the genome of the LRM mutants, DNA
631 was extracted and the genomes were sequenced as detailed in Methods. In all cases, the
632 Girr_Δ*lysF1b*-LRMs and NBJ_Δ*lysF1b*-LRMs contained the expected *lysF1b* deletion but all
633 phage also contained either nucleotide insertions, deletions or substitutions within the *lysF1a*
634 open reading frame that altered the amino acid sequence of the LysF1a protein. A summary of
635 all LRM mutants is provided in Table 3 and a schematic showing the amino acid changes to the
636 different Girr_lysF1a-LRMs is presented in Figure S13.
637 Six different mutations were identified in the ten Girr_Δ*lysF1b*-LRMs and two in the four
638 NBJ_Δ*lysF1b*-LRMs.The mutations mapped to three different domains of the LysF1a protein:
639 the N-terminal cytoplasmic domain, the first TMD or the beginning of the cytoplasmic C-terminal
640 domain. No mutants were recovered that impacted the second TMD or distal regions of the
641 cytoplasmic C-terminal domain. In the Girr LRM mutants, two different missense mutations were
642 found in TMD1 of LysF1a that result in R19H and A31T while one of the NBL LRM mutants
643 changed the charged cytoplasmic D9 to A. In addition, three G66D mutants were recovered in
644 the Girr LRMs, and three A68E mutants were recovered in the NBJ LRMs. All of these change a
645 small hydrophobic amino acid to a negatively charged amino acid just after the end of the TMD2
646 at the beginning of the cytoplasmic C-terminal domain. Finally, four mutants generate a
647 nonsense mutation that either truncates the Girr LysF1a protein after G66 or create a frame shift
648 after A63 that results in missense coding and a premature stop after amino acid 73. All LRM
649 mutations result in changes to the LyF1a protein that likely alter its conformation, thus, the
650 findings validate that the LysF1a protein can efficiently function in the lysis pathway and that the
651 protein is not exclusively an antiholin.
652

653 **Lysis Recovery Mutants Exhibit Early Lysis and Reduced Burst Size**

654 Since the LRMs generate a wild type plaque size (Figure 12A, Figure S12), it was
655 pertinent to evaluate the lysis timing in liquid culture and determine lag time and burst size. *M.*
656 *smegmatis* was infected with Girr_WT, Girr_*ΔlysF1b* and three different Girr_*ΔlysF1b*-LRMs and
657 the OD_{600} of the culture measured as described in Methods. Figure 13A shows that Girr_WT
658 triggers lysis as expected at ~110-minutes while Girr_*ΔlysF1b* causes reduced culture growth
659 but no defined triggering as also shown in Figures 9 and 10. In stark contrast, Girr_*ΔlysF1b*-
660 LRM1*,* Girr_*ΔlysF1b*-LRM2 and Girr_*ΔlysF1b*-LRM16, all trigger lysis prematurely at ~90
661 minutes and ultimately reduce the OD_{600} to the same baseline as Girr_WT. When NBJ_WT,
662 NBJ_*ΔlysF1b*, NBJ_*ΔlysF1b*-LRM1 and NBJ_*ΔlysF1b*-LRM7 were tested in the liquid lysis
663 assay, the NBJ-LRMs also trigger lysis prematurely and reduce the OD_{600} to the same level as
664 NBJ_WT (Figure 13B). To validate the early triggering time and assess its impact on burst size,
665 one-step growth curves were completed as described in Methods. Figure 13C shows a
666 representative one-step experiment with Girr_WT and two LRM mutants. Phage release from
667 Girr_*ΔlysF1b*-LRM1 and Girr_Girr_*ΔlysF1b*-LRM2 is detected by 150 minutes and plateaus by
668 200-minutes, a time point at which Girr_WT has achieved <10% burst size. The two Girr LMRs
669 average burst size is also only 95.5 +/- 12.5 PFU/cell compared to 289.6 +/- 65 PFU/cell for the
670 Girr_WT. The reduced burst size is likely the result of lysis triggering well before all phage
671 progeny have been full assembled and is consistent with reports that have evaluated early
672 triggering in *E. coli* phages [11, 12, 74]. The current results also indicate that plaque size in our
673 experimental system is not a function of burst size since a >65% reduction in burst size is still
674 able to generate wild type-sized plaques (Figure 12A,Figure S12). These findings add further
675 support to the hypothesis that the small plaque phenotypes of the various LysF1 mutants is the
676 result of inefficient cell wall lysis that hampers phage release.

677 **Analysis of *lysF1b* Phage Plaque Sizes in *M. smegmatis* Lacking the Lipoarabinomannan**
678 **Layer of the Cell Wall**

679 A recent study proposes a 1TMD protein termed LysZ may function as a spanin-like
680 protein to disrupt the integrity of the Gram-positive *Corynebacterium glutamicum* cell wall by
681 interacting with the lipoarabinomannan (LAM) layer [57]. In these studies, deletion of *lysZ* from
682 phages CL31 or Cog results in a small plaque phenotype that is rescued if phage were plated
683 on a *Corynebacteriumg glutamicum* strain that is defective in the synthesis the LAM. Since both
684 LysZ and LysF1b have a single TMD and deletion of the genes results in small plaques, it was
685 pertinent to determine whether an *M. smegmatis* strain lacking the mtpA enzyme required to
686 synthesize LAM (*M. smegmatis* ∆mtpA) [66], would complement the small plaque phenotype of
687 Girr_∆*lysF1b*. Wild type *M. smegmatis*, *M. smegmatis* ∆mtpA, and *M. smegmatis* ∆mtpA-comp
688 (∆mtpA carrying complementing mtpA expression plasmid), were grown to saturation and set to
689 OD_{600} of 2.0 prior to infection. Equal amounts of phage were used to infect and cells and
690 plaques evaluated after incubation for 48 hrs. at 37°C. Figure 14A shows that both wild type Girr
691 and Girr_∆*lysF1b* exhibit a modest but significant increase in plaque size when infected into the
692 *M. smegmatis* ∆mtpA strain compared to the wild type *M. smegmatis* or the *M. smegmatis*
693 ∆mtpA-comp strain. Girr_WT plaques increased by 1.4-fold from 2.8mm to 3.9mm while
694 Girr_∆*lysF1b* increased by 1.8-fold from 0.93mm to 1.7mm (Figure 14B). To account for the
695 possibility that the change is plaque size were caused by reduced cell growth and less *M.*
696 *smegmatis* ∆mtpA bacteria growing over the courses of the experiment, studies were repeated
697 using high density cultures at 2 x 10^8 CFU/infection. This level of bacteria will exacerbate small
698 plaque phenotypes since the increased cells enhance absorption and reduce phage diffusion
699 [27; 81-83]. In these studies, both Girr_WT and Girr_∆*lysF1b* showed similar plaques size
700 increases as the low-density experiments verifying that *M. smegmatis* lacking a formal LAM
701 layer is generally less restrictive to lysis and phage release (RSP, data not shown). Since both

702 Girr_WT and Girr_Δ*lysF1b* show increased plaque size and the plaques of Girr_Δ*lysF1b* do not
703 reach Girr_WT size, the results indicate that the lack of the LAM layer does not effectively
704 complement the deletion of *lyF1b*. This is consistent with the proposed holin function of the
705 LysF1b and supports the hypothesis that the LysF1b and LysZ proteins have distinct functions
706 in the lysis pathway in their respective bacterial hosts although holin function for LysZ has not
707 been formally evaluated.

708 **Analysis of Additional Genes Proposed to be Involved in the Lysis Pathway of F1 Cluster**
709 **Phages**

710 It is currently unknown how the various endolysins encoded by actinobacteriophages
711 gain access to the peptidoglycan layer following phage infection. Although exogenous
712 expression of the lysin A from some phages is cytotoxic to *M. smegmatis*, there is no evidence
713 of signal sequences or SAR domains in these proteins [20, 29-32]. However, *Mycobacterium sp.*
714 appear to have several different secretion systems that do not require a signal sequence [77-
715 80]. Additionally, it has been proposed that phage Ms6 encodes a small chaperone protein
716 (gp23) required for the export of Lysin A because the deletion of the gene results in a small
717 plaque phenotype [48, 50]. Since both phage Girr and NBJ encode a homolog to gp23 in the
718 same general genomic area upstream of the Lysin A (gene *29*; Figure 15A), it was of interest to
719 determine if deletion caused a lysis defect in Girr and NBJ. Figure 14D shows that Girr gp29 is
720 73 amino acids and shares 76.2% identity to Ms6 gp23 while NBJ gp29 shares 76 of 77 amino
721 acids with gp23. BRED was utilized to delete gene *29* from Girr and two independent Girr_Δ*29*
722 phage mutants were isolated (Figure 15B). Girr_Δ*29-20* and Girr__Δ*29-25* showed no lysis
723 defect when compared to Girr_WT in the liquid lysis assay (Figure 15C) and showed identical
724 plaque size to Girr_WT (Figure 15E). BRED deletion of NBJ *29* (NBJ_Δ*29*) also showed wild
725 type plaque size (Figure 15E) and no difference in liquid lysis when compared to NBJ_WT
726 (RSP, data not shown). To explore the possible interaction of the Lysin A and gp29 further, the

727 proteins were modeled using AlphaFold3. The results presented in Figures S14-16 show that all
728 models produced data with ipTM values <0.4 indicating a very low confidence in the interactions
729 of the proteins. Thus, these results suggest that gp29 from phage Girr or NBJ is not involved in
730 the lysis pathway. These finding are consistent with the lethal phenotype observed when both
731 *lysF1a* and *lysF1b* are deleted since deletion of holin genes is lethal in phages that express a
732 cytoplasmic endolysin that must exit through the holin [10-12]. If there was another gene that
733 was absolutely required for the lysis pathway in Girr and NBJ, especially one that could
734 enhance the secretion of the Lysin A in a holin-independent manner, it is unlikely that deletion of
735 *lysF1a* and *lysF1b* would be lethal. A plausible explanation for the lysis defects observed in the
736 Ms6 studies is that the method of deletion of gene *23* somehow impacted the expression of
737 Lysin A (gene *24*) to generate a lysis phenotype. Full genome sequencing data of the Ms6
738 mutants was not presented or discussed [48, 50] and the requirement of a phage encoded
739 chaperone has not been identified in any other phage.

740 **CONCLUSIONS AND IMPLICATIONS**

741 The results presented in this report identify the novel LysF1a and LysF1b proteins as
742 required holin-like components of *M. smegmatis* lysis by F1 cluster phages. The data support
743 that LysF1a and LysF1b function together as holins to time the lysis event and disrupt the PMF,
744 however, it appears that LysF1a requires the presence of the LysF1b protein to be active as a
745 holin. Holin function is based on several key findings. First, the deletion of both *lysF1a* and
746 *lysF1b* genes is lethal to phage propagation (Figure 5). This is consistent with the results from
747 *E. coli* phages where deletion of canonical holins from phages that express cytoplasmic
748 endolysins are lethal [10-12]. In addition, deletion of both the *lysF1a* and *lysF1b* genes in the F1
749 cluster phage Ms6 also appears to be lethal as no viable phage were isolated from secondary
750 plaques [48]. Second, holin function for the LysF1b protein is directly demonstrated by the ability
751 of energy poisons to trigger premature lysis in phages that do not express LysF1a (Figure 10).
752 Third, holin function is supported for LysF1b instead of releasin function because there is no

753 defined SAR-endolysins in F1 cluster phages and the energy poisons do not trigger early lysis
754 by releasin in phage Mu [18]. Finally, holin function is supported for LysF1a by the ability to
755 recover LRM mutants in the Δ*lysF1b* background of both Girr and NBJ that map to the LysF1a
756 protein and create phage that trigger lysis early but are fully lysis competent (Figure 13).
757 The 1TMD LysF1b proteins represent a new class of holins and appear to be found
758 predominantly in phages that infect Gram positive hosts. HHpred analysis shows that the
759 LysF1b proteins have a high probability hit to Pfam PF10874 (DUF2746) that contains 906
760 proteins. Within this Pfam are hits to phages that infect *Mycobacterium sp, Gordonia sp,* and
761 *Streptomyces sp* and hits to *Micromonospora sp, Rothia sp, Saccharothrix sp, Nocardia*
762 *terpenica, Propionicmonas paludicola, Microbacterium talmoniae, Xylanimonas oleitrophica and*
763 *Actinacidiphilia glaucinigra* where the later hits are likely to proteins that are encoded by
764 prophages within the host bacteria. To assess whether additional phages in the
765 Actinobacteriophage Database at PhagesDB.org express a LysF1-b-like homolog [84], phages
766 infecting *M. smegmatis* were bioinformatically evaluated as described in Methods to identify the
767 lysis cassette and associated genes that encode proteins with 1TMD. Of the ~2,600 phages in
768 the database, 80% encoded a LysF1b-like protein with an N-out-C-in membrane topology and
769 the proteins were grouped to 20 different phams based on their amino acid identity [85, 86].
770 Representative proteins from each pham are presented in Figure S17. The proteins differ in size
771 from 92-150 amino acids, have several basic amino acids after the TMD as highlighted in Figure
772 3 and have between 30%-50% DEKRH charged amino acids in the C-terminal cytoplasmic
773 domain (Figure S17). Multiple sequence alignment indicates minimal amino acid identity
774 between the proteins (Figure S18) and the alignment also failed to identify any small regions of
775 high identity that might serve as functional domains. Thus, while most phages that infect *M.*
776 *smegmatis* in the PhagesDB.org database express a LysF1b-like protein, it is unclear whether
777 they all function like the LysF1b proteins from Girr and NBJ.

778 Since deletion of both *lysF1a* and *lysF1b* genes in F1 phages is lethal and the LysF1b
779 protein clearly can function independent of the LysF1a, what then is the function of the 2TMD
780 LysF1a proteins in the lysis pathway? As discussed throughout this report, a role of LysF1a as a
781 type II pinholin is not supported by the sequence data (Figure 3), or by AlphaFold3 models
782 (Figure S7). In fact, the amino acid sequence data and lack of lysis function in the absence of
783 LysF1b, better supports LysF1a as an inactive antiholin. However, deletion of the *lysF1a* gene
784 results in a lysis triggering *delay* in both Girr_Δ*lysF1b* and NBJ_ Δ*lysF1b* with the later delayed
785 over 60 minutes compared to NBJ_WT (Figure 8). A lysis delay is not consistent with the
786 function of LysF1a as a true antiholin to the LysF1b, since it would be expected that deletion of
787 the antiholin would result in *early* host lysis by Girr_Δ*lysF1a* or Girr_Δ*lysF1a* since the LysF1b
788 would not be inhibited from forming active multimers as shown for lambda S_{105} and phage 21
789 $S^{21}68$ [10-12]. The data also demonstrate that expression of Girr or NBJ LysF1a in the absence
790 of the LysF1b results in cell death with release of ATP, but that actual lysis and shape change of
791 the bacteria is not detected by changes to the OD_{600} (Figure 8). These results suggest that
792 expression of Girr or NBJ LysF1a also will ultimately disrupt the membrane to destroy the PMF,
793 but whatever lesion is produced cannot effectively facilitate the release of the endolysins and/or
794 phage particles. In this context, the key findings are 1) that destabilization of the PMF alone is
795 not sufficient to “activate” LysF1a into a lesion that supports wild type lysis or phage release
796 (Figure 10), and 2) that LRMs can be recovered in the Δ*lysF1b* background that have point
797 mutations LysF1a that result in a fully lysis competent LysF1a protein that happens to trigger
798 premature (i.e. unregulated) lysis (Figure 13). These findings suggest that amino acid changes
799 to the protein may induce conformational changes to the LysF1a that allow it to fully support
800 bacterial lysis and phage release in the absence of the LysF1b. Thus, an attractive working
801 model is that LysF1a is not an antiholin to LysF1b but simply is not lysis active without LysF1b.
802 Therefore, as expression of both proteins increases following infection, they reach a

803 concentration at which they can formally interact, and this interaction facilitates conformational
804 changes in the LysF1a that allow it to become active in lysis. The two proteins then function
805 together to facilitate the release of endolysins and/or phage particles. Such a model would be
806 like the holin/antiholin system in phage lambda and phage 21 where the phages express both
807 active holins and inactive antiholins and triggering results in an instantaneous conversion of all
808 proteins to active holins [10-12].

809 Currently, it is unclear how the LysF1a and LysF1b proteins interact and whether both
810 proteins together actively participate in the creation a heteromeric lesion the inner membrane.
811 Clearly, LysF1b alone can trigger lysis and facilitate significant phage release, but as stated
812 above, lysis timing and the efficiency of phage release are still not optimal. There is also no
813 precedent for two structurally distinct TMD proteins functioning together to make a lesion. The
814 lysis pathway of phage P2 utilizes two distinct proteins, holin Y and antiholin LysA, but LysA
815 protein appears to be fully regulatory to holin Y and is not converted into an active holin like the
816 antiholins S_{107} or $S^{21}71$ [11, 55, 56]. Thus, the interaction of two distinct holin monomers that
817 have different membrane topologies is unprecedented and will require direct study of LysF1a
818 and LysF1b proteins within membranes to resolve the structure. Such work could also directly
819 address whether the LysF1b also has interactions with cell wall components to facilitate phage
820 release as suggested for the LysZ proteins of *Corynebacterium* phages [57]. Whether the other
821 Mycobacteriophages that express different variants of the LysF1a and LysF1b proteins also
822 utilize them in the same way as Girr and NBJ will require additional deletion and
823 complementation studies. The current study therefore provides a framework to evaluate lysis
824 under physiological conditions in Gram-positive hosts. It is exciting to speculate that due to the
825 presence of *lysF1*-like and *lysZ*-like genes in so many phages, it may be that the phages that
826 infect Gram-positive hosts use a similar set of tools to complete the lysis pathway through
827 distinct molecular mechanisms just as observed for phages that infect *E. coli.*
828

829 **DATA AVAILABILITY STATEMENT**

830 All recombinant phage and expression plasmids used in this study are available upon request.
831 The authors affirm that all data necessary for confirming the conclusions of this article are
832 represented fully within the article and its tables and figures. Extended data, including plasmid
833 Sanger sequencing data and confirmatory cytotoxicity assay data for all Girr and NBJ pExTra
834 constructs can be found at the SEA-GENES project open access database GenesDB
835 (https://genesdb.org). To access these data on genesDB.org, any user can register for a free
836 account, and once logged in to this account, navigate from the home page to Cluster F1 phage
837 Girr or NBJ. Full genome sequences of Girr and NBJ are available in GenBank through
838 accession numbers MH669003 and MH399784, respectively.

839 **ACKNOWLEDGMENTS**

840 We are grateful to the members of the Science Education Alliance for their invaluable research
841 support and for supplying phage and plasmid reagents, particularly Dainelle Heller, Viknesh
842 Sivanathan, Graham Hatfull, Deborah Jacobs-Sera, Becky Garlena and Dan Russell. We also
843 thank the Pittsburgh Bacteriophage Institute for genome sequencing of the phages described in
844 this study. We want to thank A. McKitterick for helpful discussions regarding LysZ. We want to
845 thank Y. Morita for generously sending the ΔmtpA *M. smegmatis* strains.

846 **FUNDING**

847 This project was funded in part by an Undergraduate Grants in Aid for Research from USF
848 Chapter of Sigma Xi to KRH and a USF Internal Proposal Enhancement Grant to RSP.

849 **REFERENCS**

850 1. Mushegian AR. Are There 10(31) Virus Particles on Earth, or More, or Fewer? J Bacteriol.
851 2020;202(9).
852 2. Oliveira H, Melo LD, Santos SB, Nobrega FL, Ferreira EC, Cerca N, et al. Molecular aspects
853 and comparative genomics of bacteriophage endolysins. J Virol. 2013;87(8):4558-70.

854 3. Ryan GL, Rutenberg AD. Clocking out: modeling phage-induced lysis of Escherichia coli. J
855 Bacteriol. 2007;189(13):4749-55.
856 4. Pang T, Fleming TC, Pogliano K, Young R. Visualization of pinholin lesions in vivo. Proc Natl
857 Acad Sci U S A. 2013;110(22):E2054-63.
858 5. Savva CG, Dewey JS, Deaton J, White RL, Struck DK, Holzenburg A, et al. The holin of
859 bacteriophage lambda forms rings with large diameter. Mol Microbiol. 2008;69(4):784-
860 93.
861 6. Savva CG, Dewey JS, Moussa SH, To KH, Holzenburg A, Young R. Stable micron-scale
862 holes are a general feature of canonical holins. Mol Microbiol. 2014;91(1):57-65.
863 7. Summer EJ, Berry J, Tran TA, Niu L, Struck DK, Young R. Rz/Rz1 lysis gene equivalents in
864 phages of Gram-negative hosts. J Mol Biol. 2007;373(5):1098-112.
865 8. Rajaure M, Berry J, Kongari R, Cahill J, Young R. Membrane fusion during phage lysis. Proc
866 Natl Acad Sci U S A. 2015;112(17):5497-502.
867 9. Berry J, Rajaure M, Pang T, Young R. The spanin complex is essential for lambda lysis. J
868 Bacteriol. 2012;194(20):5667-74.
869 10. Young R. Phage lysis: three steps, three choices, one outcome. J Microbiol.
870 2014;52(3):243-58.
871 11. Cahill J, Young R. Phage Lysis: Multiple Genes for Multiple Barriers. Adv Virus Res.
872 2019;103:33-70.
873 12. Cahill J, Holt A, Theodore M, Moreland R, O'Leary C, Martin C, et al. Spatial and temporal
874 control of lysis by the lambda holin. mBio. 2024;15(2):e0129023.
875 13. Park T, Struck DK, Dankenbring CA, Young R. The pinholin of lambdoid phage 21: control
876 of lysis by membrane depolarization. J Bacteriol. 2007;189(24):9135-9.
877 14. Barenboim M, Chang CY, dib Hajj F, Young R. Characterization of the dual start motif of a
878 class II holin gene. Mol Microbiol. 1999;32(4):715-27.

879 15. Blasi U, Young R. Two beginnings for a single purpose: the dual-start holins in the
880 regulation of phage lysis. Mol Microbiol. 1996;21(4):675-82.
881 16. Ramanculov E, Young R. An ancient player unmasked: T4 rI encodes a t-specific antiholin.
882 Mol Microbiol. 2001;41(3):575-83.
883 17. Ramanculov E, Young R. Genetic analysis of the T4 holin: timing and topology. Gene.
884 2001;265(1-2):25-36.
885 18. Chamblee JS, Ramsey J, Chen Y, Maddox LT, Ross C, To KH, et al. Endolysin Regulation
886 in Phage Mu Lysis. mBio. 2022;13(3):e0081322.
887 19. Raman SK, Siva Reddy DV, Jain V, Bajpai U, Misra A, Singh AK. Mycobacteriophages:
888 therapeutic approach for mycobacterial infections. Drug Discov Today.
889 2024;29(7):104049.
890 20. Payne KM, Hatfull GF. Mycobacteriophage endolysins: diverse and modular enzymes with
891 multiple catalytic activities. PLoS One. 2012;7(3):e34052.
892 21. Schmelcher M, Donovan DM, Loessner MJ. Bacteriophage endolysins as novel
893 antimicrobials. Future Microbiol. 2012;7(10):1147-71.
894 22. Arenskotter M, Broker D, Steinbuchel A. Biology of the metabolically diverse genus
895 Gordonia. Appl Environ Microbiol. 2004;70(6):3195-204.
896 23. Goodfellow M, Jones AL. Corynebacteriales ord. nov. Bergey's Manual of Systematics of
897 Archaea and Bacteria. 2015. p. 1-14.
898 24. Brennan PJ. Structure, function, and biogenesis of the cell wall of Mycobacterium
899 tuberculosis. Tuberculosis (Edinb). 2003;83(1-3):91-7.
900 25. Hart EM, Bernhardt TG. The mycomembrane. Curr Biol. 2025;35(3):R85-R6.
901 26. Catalao MJ, Pimentel M. Mycobacteriophage Lysis Enzymes: Targeting the Mycobacterial
902 Cell Envelope. Viruses. 2018;10(8).
903 27. Payne K, Sun Q, Sacchettini J, Hatfull GF. Mycobacteriophage Lysin B is a novel
904 mycolylarabinogalactan esterase. Mol Microbiol. 2009;73(3):367-81.

905 28. Marinelli LJ, Piuri M, Swigonova Z, Balachandran A, Oldfield LM, van Kessel JC, et al.
906 BRED: a simple and powerful tool for constructing mutant and recombinant
907 bacteriophage genomes. PLoS One. 2008;3(12):e3957.
908 29. Joshi H, Seniya SP, Suryanarayanan V, Patidar ND, Singh SK, Jain V. Dissecting the
909 structure-function relationship in lysozyme domain of mycobacteriophage D29-encoded
910 peptidoglycan hydrolase. FEBS Lett. 2017;591(20):3276-87.
911 30. Singh AK, Gangakhedkar R, Thakur HS, Raman SK, Patil SA, Jain V. Mycobacteriophage
912 D29 Lysin B exhibits promising anti-mycobacterial activity against drug-resistant
913 Mycobacterium tuberculosis. Microbiol Spectr. 2023;11(6):e0459722.
914 31. Pohane AA, Joshi H, Jain V. Molecular dissection of phage endolysin: an interdomain
915 interaction confers host specificity in Lysin A of Mycobacterium phage D29. J Biol Chem.
916 2014;289(17):12085-95.
917 32. Nair G, Jain V. An intramolecular cross-talk in D29 mycobacteriophage endolysin governs the
918 lytic cycle and phage-host population dynamics. Sci. Adv.2024;10(6):
919 33. Gil F, Catalao MJ, Moniz-Pereira J, Leandro P, McNeil M, Pimentel M. The lytic cassette of
920 mycobacteriophage Ms6 encodes an enzyme with lipolytic activity. Microbiology
921 (Reading). 2008;154(Pt 5):1364-71.
922 34. Gil F, Grzegorzewicz AE, Catalao MJ, Vital J, McNeil MR, Pimentel M. Mycobacteriophage
923 Ms6 LysB specifically targets the outer membrane of Mycobacterium smegmatis.
924 Microbiology (Reading). 2010;156(Pt 5):1497-504.
925 35. Loessner MJ, Gaeng S, Wendlinger G, Maier SK, Scherer S. The two-component lysis
926 system of Staphylococcus aureus bacteriophage Twort: a large TTG-start holin and an
927 associated amidase endolysin. FEMS Microbiol Lett. 1998;162(2):265-74.
928 36. Kwan T, Liu J, DuBow M, Gros P, Pelletier J. The complete genomes and proteomes of 27
929 Staphylococcus aureus bacteriophages. Proc Natl Acad Sci U S A. 2005;102(14):5174-
930 9.

931 37. Vybiral D, Takac M, Loessner M, Witte A, von Ahsen U, Blasi U. Complete nucleotide
932 sequence and molecular characterization of two lytic Staphylococcus aureus phages:
933 44AHJD and P68. FEMS Microbiol Lett. 2003;219(2):275-83.
934 38. Godinho LM, El Sadek Fadel M, Monniot C, Jakutyte L, Auzat I, Labarde A, et al. The
935 Revisited Genome of Bacillus subtilis Bacteriophage SPP1. Viruses. 2018;10(12).
936 39. Escobedo S, Campelo AB, Wegmann U, Garcia P, Rodriguez A, Martinez B. Insight into the
937 Lytic Functions of the Lactococcal Prophage TP712. Viruses. 2019 ;11(10).
938 40. Sao-Jose C, Parreira R, Vieira G, Santos MA. The N-terminal region of the Oenococcus
939 oeni bacteriophage fOg44 lysin behaves as a bona fide signal peptide in Escherichia coli
940 and as a cis-inhibitory element, preventing lytic activity on oenococcal cells. J Bacteriol.
941 2000;182(20):5823-31.
942 41. Gindreau E, Lonvaud-Funel A. Molecular analysis of the region encoding the lytic system
943 from Oenococcus oeni temperate bacteriophage phi 10MC. FEMS Microbiol Lett.
944 1999;171(2):231-8.
945 42. Nelson D, Schuch R, Zhu S, Tscherne DM, Fischetti VA. Genomic sequence of C1, the first
946 streptococcal phage. J Bacteriol. 2003;185(11):3325-32.
947 43. Pope WH, Mavrich TN, Garlena RA, Guerrero-Bustamante CA, Jacobs-Sera D,
948 Montgomery MT, et al. Bacteriophages of Gordonia spp. Display a Spectrum of Diversity
949 and Genetic Relationships. mBio. 2017;8(4).
950 44. Pollenz RS, Bland J, Pope WH. Bioinformatic characterization of endolysins and holin-like
951 membrane proteins in the lysis cassette of phages that infect Gordonia rubripertincta.
952 PLoS One. 2022;17(11):e0276603.
953 45. McGarrah CEE, Algarin-Martinez ED, Cavasini MED, Correa V, Danielson DF, Dean WR, et
954 al. Isolation and Annotation of Azira, a CT Cluster Phage That Infects Gordonia
955 rubripertincta. Microbiol Resour Announc. 2023;12(7):e0034723.

956 46. Dedrick RM, Marinelli LJ, Newton GL, Pogliano K, Pogliano J, Hatfull GF. Functional
957 requirements for bacteriophage growth: gene essentiality and expression in
958 mycobacteriophage Giles. Mol Microbiol. 2013;88(3):577-89.
959 47. Sandoval AM, Abram AM, Alhabib ZM, Antonyan AS, Brikho SM, Buhay SI, et al. Complete
960 Genome Sequences of Cluster G Mycobacteriophage Darionha, Cluster A
961 Mycobacteriophage Salz, and Cluster J Mycobacteriophage ThreeRngTarjay. Microbiol
962 Resour Announc. 2020;9(20).
963 48. Catalao MJ, Gil F, Moniz-Pereira J, Pimentel M. Functional analysis of the holin-like proteins
964 of mycobacteriophage Ms6. J Bacteriol. 2011;193(11):2793-803.
965 49. Garcia M, Pimentel M, Moniz-Pereira J. Expression of Mycobacteriophage Ms6 lysis genes
966 is driven by two sigma(70)-like promoters and is dependent on a transcription
967 termination signal present in the leader RNA. J Bacteriol. 2002;184(11):3034-43.
968 50. Catalao MJ, Gil F, Moniz-Pereira J, Pimentel M. The mycobacteriophage Ms6 encodes a
969 chaperone-like protein involved in the endolysin delivery to the peptidoglycan. Mol
970 Microbiol. 2010;77(3):672-86.
971 51. Bavda VR, Jain V. Deciphering the Role of Holin in Mycobacteriophage D29 Physiology.
972 Front Microbiol. 2020;11:883.
973 52. Bavda VR, Yadav A, Jain V. Decoding the molecular properties of mycobacteriophage D29
974 Holin provides insights into Holin engineering. J Virol. 2021;95(10).
975 53. Kamilla S, Jain V. Mycobacteriophage D29 holin C-terminal region functionally assists in
976 holin aggregation and bacterial cell death. FEBS J. 2016;283(1):173-90.
977 54. Ford ME, Sarkis GJ, Belanger AE, Hendrix RW, Hatfull GF. Genome structure of
978 mycobacteriophage D29: implications for phage evolution. J Mol Biol. 1998;279(1):143-
979 64.
980 55. To KH, Dewey J, Weaver J, Park T, Young R. Functional analysis of a class I holin, P2 Y. J
981 Bacteriol. 2013;195(6):1346-55.

982 56. Christie GE, Calendar R. Bacteriophage P2. Bacteriophage. 2016;6(1):e1145782.
983 57. McKitterick AC, Lyerly EW, Bernhardt TG. Bacteriophages target membrane-anchored
984 glycopolymers to promote host cell lysis and progeny release. bioRxiv.
985 2025:2025.06.24.661397.
986 58. Hallgren J, Tsirigos KD, Pedersen MD, Almagro Armenteros JJ, Marcatili P, Nielsen H, et al.
987 DeepTMHMM predicts alpha and beta transmembrane proteins using deep neural
988 networks. bioRxiv. 2022:2022.04.08.487609.
989 59. Tsirigos KD, Peters C, Shu N, Kall L, Elofsson A. The TOPCONS web server for consensus
990 prediction of membrane protein topology and signal peptides. Nucleic Acids Res.
991 2015;43(W1):W401-7.
992 60. Almagro Armenteros JJ, Tsirigos KD, Sonderby CK, Petersen TN, Winther O, Brunak S, et
993 al. SignalP 5.0 improves signal peptide predictions using deep neural networks. Nat
994 Biotechnol. 2019;37(4):420-3.
995 61. Juncker AS, Willenbrock H, Von Heijne G, Brunak S, Nielsen H, Krogh A. Prediction of
996 lipoprotein signal peptides in Gram-negative bacteria. Protein Sci. 2003;12(8):1652-62.
997 62. Soding J, Biegert A, Lupas AN. The HHpred interactive server for protein homology
998 detection and structure prediction. Nucleic Acids Res. 2005;33(Web Server
999 issue):W244-8.
1000 63. Abramson J, Adler J, Dunger J, Evans R, Green T, Pritzel A, et al. Accurate structure
1001 prediction of biomolecular interactions with AlphaFold 3. Nature. 2024;630(8016):493-
1002 500.
1003 64. Madeira F, Madhusoodanan N, Lee J, Eusebi A, Niewielska A, Tivey ARN, Lopez, R,
1004 Butcher S. The EMBL-EBI Job Dispatcher sequence analysis tools framework in 2024.
1005 Nucleic acids research. 2024;52(W1):W521–W525.
1006

1007 65. Snapper SB, Melton RE, Mustafa S, Kieser T, Jacobs WR, Jr. Isolation and characterization
1008 of efficient plasmid transformation mutants of Mycobacterium smegmatis. Mol Microbiol.
1009 1990;4(11):1911-9.
1010 66. Sparks IL, Kado T, Prithviraj M, Nijjer J, Yan J, Morita YS. Lipoarabinomannan mediates
1011 localized cell wall integrity during division in mycobacteria. Nat Commun.
1012 2024;15(1):2191.
1013 67. Heller D, Amaya I, Mohamed A, Ali I, Mavrodi D, Deighan P, et al. Systematic
1014 overexpression of genes encoded by mycobacteriophage Waterfoul reveals novel
1015 inhibitors of mycobacterial growth. G3 (Bethesda). 2022;12(8).
1016 68. Pollenz RS, Barnhill K, Biggs A, Bland J, Carter V, Chase M, et al. A genome-wide
1017 cytotoxicity screen of cluster F1 mycobacteriophage Girr reveals novel inhibitors of
1018 Mycobacterium smegmatis growth. G3 (Bethesda). 2024;14(5).
1019 69. Wise B, Edwards K, Jirsa C, [student authors], Kanther M, Payne K, Pollenz RS, Heller DM.
1020 Identification and characterization of host-modulating effectors encoded by the Cluster F1
1021 mycobacteriophage NormanBulbieJr. bioRxiv 2025.
1022 70. van Kessel JC, Hatfull GF. Mycobacterial recombineering. Methods Mol Biol. 2008;435:203-
1023 15.
1024 71. Gordon D, Abajian C, Green P. Consed: a graphical tool for sequence finishing. Genome
1025 Res. 1998;8(3):195-202.
1026 72. Russell DA. Sequencing, Assembling, and Finishing Complete Bacteriophage Genomes.
1027 Methods Mol Biol. 2018;1681:109-25.
1028 73. Schneider CA, Rasband WS, Eliceiri KW. NIH Image to ImageJ: 25 years of image analysis.
1029 Nat Methods. 2012;9(7):671-5.
1030 74. Pang T, Park T, Young R. Mutational analysis of the S21 pinholin. Mol Microbiol.
1031 2010;76(1):68-77.

1032 75. Park T, Struck DK, Deaton JF, Young R. Topological dynamics of holins in programmed
1033 bacterial lysis. Proc Natl Acad Sci U S A. 2006;103(52):19713-8.
1034 76. Doermann AH. The intracellular growth of bacteriophages. I. Liberation of intracellular
1035 bacteriophage T4 by premature lysis with another phage or with cyanide. J Gen Physiol.
1036 1952;35(4):645-56.
1037 77. Rigel NW, Gibbons HS, McCann JR, McDonough JA, Kurtz S, Braunstein M. The Accessory
1038 SecA2 System of Mycobacteria Requires ATP Binding and the Canonical SecA1. J Biol
1039 Chem. 2009;284(15):9927-9936.
1040 78. Abdallah A, Gey van Pittius N, DiGiuseppe Champion P, Cox J, Luirink J, et. al. Type VII
1041 secretion — mycobacteria show the way. Nat Rev Microbiol. 2007;5:883–891.
1042 79. Bendtsen JD, Kiemer L, Fausbøll A, Brunak S. Non-classical protein secretion in bacteria.
1043 BMC Microbiol. 2005;5:58.
1044 80. Zhang Z, Dong L, Li X, Deng T, Wang Q. The PE/PPE family proteins of Mycobacterium
1045 tuberculosis: evolution, function, and prospects for tuberculosis control. Front. Immunol.
1046 2025;16:1606311.
1047 81. Ameh EM, Tyrrel S, Harris JA, Pawlett M, Orlova EV, Ignatiou A, et al. Lysis Performance of
1048 Bacteriophages with Different Plaque Sizes and Comparison of Lysis Kinetics After
1049 Simultaneous and Sequential Phage Addition. Phage (New Rochelle). 2020;1(3):149-57.
1050 82. Abedon ST, Yin J. Bacteriophage plaques: theory and analysis. Methods Mol Biol.
1051 2009;501:161-74.
1052 83. Dennehy JJ, Abedon ST, Turner PE. Host density impacts relative fitness of bacteriophage
1053 Phi6 genotypes in structured habitats. Evolution. 2007;61(11):2516-27.
1054 84. Russell DA, Hatfull GF. PhagesDB: the actinobacteriophage database. Bioinformatics.
1055 2017;33(5):784-6.

1056 85. Gauthier CH, Cresawn SG, Hatfull GF. 2022. PhaMMseqs: a new pipeline for constructing
1057 phage gene phamilies using MMseqs2. G3 Genes Genomes Genetics.
1058 2022;12(11):jkac233.

1059 86. Gauthier CH, Hatfull GF. PhamClust: a phage genome clustering tool using proteomic
1060 equivalence. mSystems. 2023;8(5):e00443-23.

1061 **FIGURE LEGANDS**

1062

1063 **Figure 1. Lysis cassette organization of Girr and NormanBulbieJr (NBJ).** Predicted protein
1064 coding genes are shown as colored boxes. The genomic location is represented by the ruler,
1065 and the numbers represent the kilobase from nucleotide 1. Both lysis cassette regions are
1066 located upstream of the *tape measure* and *minor tail* genes. Genes above the genome are
1067 transcribed in the forward direct and genes below in the reverse direction. Genes with the same
1068 color encode proteins that are grouped to the same pham. Pink shading indicated nucleotide
1069 identity >90% in the shaded region. The *lysin A, lysin B,* 2TMD *lysF1a and* 1TMD *lysF1b* genes
1070 are identified. NKF = genes with no know function; *HNH* = HNH endonuclease.

1071

1072 **Figure 2. Amino acid sequence and topology of Girr and NBJ LysF1a proteins and**
1073 **comparison to phage 21 S^{21} pinholin**. **A.** The amino acid sequences of Girr and NBJ LysF1a
1074 showing the location of the predicted TMDs and charged amino acids. **B.** The amino acid
1075 sequence of phage 21 $S^{21}68$ holin, $S^{21}71$ antiholin and $S^{21}68_{IRS}$ showing the location of the
1076 predicted TMDs and charged amino acids. **C.** Predicted membrane topology of Girr LysF1a,
1077 $S^{21}68_{IRS}$ and the proposed topology of the $S^{21}68$ holin homodimer with cytoplasmic TMD1.

1078

1079 **Figure 3. Amino acid sequence and topology of lysis proteins with 1TMD**. **A.** The amino
1080 acid sequences of Girr LysF1b, NBJ LysF1b, Waterfoul gp32 and Mu releasin showing the
1081 location of the predicted TMD and the charged amino acids. **B.** AlphaFold3 structural
1082 predictions and membrane topologies of 1TMD proteins involved in lysis. pTM values: Mu, 0.51;
1083 NBJ LysF1b, 0.40; Girr LysF1b, 0.41; Rz, 0.57; T, 0.74. **C.** Predicted topologies of Girr LysF1b
1084 and Waterfoul gp32.

1085

1086 **Figure 4. Deletion of Girr *lysF1a* and *lysF1b*. A.** Genomic structure and PCR primer set
1087 locations in Girr gene deletion mutants. Primer set 1 (P1) uses primers Girr-FL_*lysF1a* (F and
1088 R) and generates a 755bp fragment in Girr_WT and 487bp with *lysF1a* deletion. Primer set 2
1089 (P2) uses primers Girr-FL_*lysF1b* (F and R) and generates a 933bp fragment in Girr_WT and
1090 594bp with *lysF1b* deletion. Primer set 3 (P3) uses the forward Girr-FL_*lysF1a* and reverse Girr-
1091 FL_*lysF1b* and generates a 1189bp fragment in Girr_WT and either 921bp with *lysF1a* deletion
1092 or 818b with *lysF1b* deletion. **B.** PCR verification of high titer lysates of Girr_WT, Girr_Δ*lysF1a*
1093 and Girr_Δ*lysF1b* using the indicated primer sets. PCR band sizes are identified and show
1094 correct deletions of the indicated genes.
1095
1096 **Figure 5. Deletion of both Girr *lysF1a* and *lysF1b*. A**. Schematic showing experimental
1097 procedure. **B.** DADA PCR was carried out on the indicated samples as described in Methods.
1098 Negative control Girr_lysF1a shown in lanes 1 and 7. Positive control is the 1° plaque pick with
1099 the Girr_lysF1a/lysF1b phage and 325bp DADA band (+DADA) is shown in lanes 2 and 11.
1100 Lanes 3-6 show the DADA PCR screen of 2° lysates harvested from non-complementing *M.*
1101 *smegmatis* that contained the indicated number of plaques (PFU). Lanes 8-10 show DADA PCR
1102 screen of 2° lysates harvested from complementing *M. smegmatis* carrying pExTra-Girr*34*. Note
1103 the lack of a positive DADA band in all samples plated on non-complementing *M. smegmatis*.
1104
1105 **Figure 6 Plaque sizes in Girr_WT, Girr_Δ*lysF1a* and Girr_Δ*lysF1b*.** *M. smegmatis* was
1106 infected with identical numbers of phage and detailed in Methods and plaque size determined
1107 after 36 hrs. of growth at 37°C. Scale = 1cm. Plaque volume schematics are presented to
1108 illustrate the plaque size differences.
1109

1110 **Figure 7. Complementation of plaque phenotype in Girr_Δ*lysF1b*. A.** Plaque assays were
1111 completed with *M. smegmatis* using Girr_WT or Girr_Δ*lysF1b* as described in Methods. Plaque
1112 assays were completed with *M. smegmatis* complementing strains carrying the indicated
1113 pExTra-Waterfoul expression plasmids using Girr_Δ*lysF1b* as described in Methods. Plaques
1114 were evaluated following incubation at 37°C for 36 hrs. Plaques sizes were quantified using
1115 ImageJ and the average diameter +/- standard deviation for > 50 plaques is shown. * =
1116 statistically different from Girr_WT, p <*0.0001*. ** = statistically different from Girr_Δ*lysF1b*
1117 infected on *M. smegmatis* with pExTra Waterfoul_*32* with no aTc, p <*0.0001*. Scale = 1cm. B.
1118 Plaque assays were completed with *M. smegmatis* using Girr_WT or Girr_Δ*lysF1b* as described
1119 in Methods. Plaque assays were completed with *M. smegmatis* complementing strains carrying
1120 the indicated pExTra-Waterfoul expression plasmids using Girr_Δ*lysF1b* as described in
1121 Methods. Plaques were evaluated following incubation at 37°C for 48 hrs. Plaques sizes were
1122 quantified using ImageJ and the average diameter +/- standard deviation for > 50 plaques is
1123 shown * = statistically different from Girr_WT, *p <0.0001*. ** = statistically different from
1124 Girr_Δ*lysF1b* infected on *M. smegmatis* with pExTra01, *p <0.0001*. Scale = 1cm.
1125
1126 **Figure 8. Complementation of plaque phenotype in Girr_Δ*lysF1a*.** Plaque assays were
1127 completed with *M. smegmatis* using Girr_WT or Girr_Δ*lysF1a* as described in Methods. Plaque
1128 assays were completed with *M. smegmatis* complementing strains carrying pExTra-Girr_*34*
1129 expression plasmid using Girr_Δ*lysF1a*as described in Methods. Plaques were evaluated
1130 following incubation at 37°C for 48 hrs. Plaques sizes were quantified using ImageJ and the
1131 average diameter +/- standard deviation for > 50 plaques is shown. * = statistically different from
1132 Girr_WT, *p <0.0001*. ** = statistically different from Girr_Δ*lysF1a* infected on *M. smegmatis* with
1133 pExTra-Girr_*34* with no aTc, *p <0.0001*. Scale = 1cm.
1134

1135 **Figure 9. Liquid lysis assay and ATP release from *M. smegmatis* after infection.** At T_0 a log
1136 growth culture of *M. smegmatis* at an OD_{600} of ~0.25 was infected with the indicated phage at
1137 an MOI of 10:1 and incubated at 37°C for 30 minutes without shaking. Control cultures (no
1138 phage) did not receive phage. At T_{30} minutes the culture was constantly shaken a 225rpm,
1139 aliquots removed at the indicated times and bacterial growth evaluated at OD_{600}. Open white
1140 arrow shows the 30-minute infection time. **A.** Representative results following infection with
1141 Girr_WT, Girr_Δ*lysF1a* and Girr_Δ*lysF1b*. **B**. Representative results following infection with
1142 NBJ_WT, NBJ_Δ*lysF1a* and NBJ_Δ*lysF1b.* **C.** Samples of culture were removed from the
1143 cultures represented in A and B at the times indicated by the solid black triangle on the x axis.
1144 The presence of ATP was evaluated as described in Methods.
1145
1146 **Figure 10. Energy poisons trigger early lysis in phage expressing LysF1b but not LysF1a.**
1147 At T_0 a log growth culture of *M. smegmatis* at an OD_{600} of ~0.25 was infected with the indicated
1148 phage at an MOI of 10:1 and incubated at 37°C for 30 minutes without shaking. Control cultures
1149 (no phage) did not receive phage. At T_{30} minutes the culture was constantly shaken a 225rpm,
1150 aliquots removed at the indicated times and bacterial growth evaluated at OD_{600}. **A**.
1151 Representative results following infection with Girr_WT, and Girr_Δ*lysF1a*. KCN (final
1152 concentration of 10mM) was added to a culture infected with Girr_Δ*lysF1a* and an uninfected
1153 culture at 110 minutes (open arrow). **B**. Representative results following infection with NBJ_WT,
1154 and NBJ_Δ*lysF1a.* KCN (final concentration of 10mM) was added to a culture infected with
1155 NBJ_Δ*lysF1a* and uninfected culture at 120 minutes (open arrow). **C.** Representative results
1156 following infection with Girr_WT, and Girr_Δ*lysF1b*. KCN (final concentration of 10mM) or $CHCl_3$
1157 (final concentration 1%) was added to cultures infected with Girr_Δ*lysF1b* and uninfected
1158 cultures at 180 minutes (open arrow). **D**. Representative results following infection with
1159 NBJ_WT, and NBJ_Δ*lysF1b.* KCN (final concentration of 10mM) or $CHCl_3$ (final concentration

1160 1%) was added to cultures infected with NBJ_Δ*lysF1b* and uninfected cultures at 180 minutes
1161 (open arrow).
1162
1163 **Figure 11. One-step growth curves of *M. smegmatis* infected with Girr_Δ*lysF1a* and**
1164 **Girr_Δ*lysF1b*. A**. One-step growth curves using Girr_WT, Girr_Δ*lysF1a* and Girr_Δ*lysF1b* were
1165 completed as described in Methods. Each time point represents the average and standard
1166 deviation from 3 different experiments. **B**. The data for Girr_Δ*lysF1b* from panel A replotted with
1167 a different Y axis than used in A. **C**. Burst size was determined as described in Methods. The
1168 average bust size +/- standard deviation is from three different experiments and represents the
1169 average of all points once the curve reached a plateau.
1170
1171 **Figure 12. Isolation of Girr_Δ*lysF1b*-LRM mutants**. **A**. *M. smegmatis* was infected with
1172 GirrΔ*lysF1b,* plate lysates recovered from the plaque assay and *M. smegmatis* infected with the
1173 recovered phage. Panel A shows a representative plaque assay following the second round of
1174 infection. A large plaque is circled. **B**. Phage were isolated from the large plaque in A, serial
1175 diluted and used for plaque assay. Plates were incubated at 37°C for 36 hrs. **C**. Plaque assay
1176 from Girr_WT phage. Plates were incubated at 37°C for 36 hrs. Scale bar = 1cm in all images.
1177
1178 **Figure 13. Liquid lysis and one-step assay of Girr and NBJ LRM mutants.** At T_0 a log
1179 growth culture of *M. smegmatis* at an OD_{600} of ~0.25 was infected with the indicated phage at
1180 MOI 10:1 for 30 minutes at 37°C without shaking. Control cultures (no phage) did not receive
1181 phage. At T_{30} minutes the culture was constantly shaken a 225rpm and aliquots removed over
1182 time. *M. smegmatis* growth was evaluated at OD_{600}. **A**. Representative results following infection
1183 with Girr_WT and indicated LRM mutants. **B**. Representative results following infection with
1184 NBJ_WT and indicated LRM mutants **C.** One-step growth curves using Girr_WT and

1185 Girr_Δ*lysF1b*-LRM1 and Girr_Δ*lysF1b*-LRM2 were completed as described in Methods. Each
1186 time point represents the average and standard deviation from 3 different experiments.
1187
1188 **Figure 14. Analysis of *lysF1b* phage plaque sizes in *M. smegmatis* lacking the**
1189 **lipoarabinomannan layer. A**. Representative plaque assays using Wild type *M. smegmatis, M.*
1190 *smegmatis* ΔmtpA-comp or *M. smegmatis* ΔmtpA cultures infected with the same amount of
1191 Girr_WT or Girr_Δ*lysF1b* and incubated for 48 hrs. at 37°C. Ruler = 1cm. **B**. Plaque sizes were
1192 determined as described in Methods. The average plaque diameter +/- standard deviation for 25
1193 plaques is shown.
1194
1195 **Figure 15. Analysis of NKF gene *29*. A**. Gene organization of Girr, NBJ and Ms6 lysis cassette
1196 region. Predicted protein coding genes are shown as colored boxes. The genomic location is
1197 represented by the ruler, and the numbers represent the kilobase from nucleotide 1. Genes
1198 above the genome are transcribed in the forward direct and genes below in the reverse
1199 direction. Genes with the same color encode proteins that are grouped to the same pham. Pink
1200 shading indicated nucleotide identity >90% in the shaded region. *NKF* = Girr_*29*, NBJ_*29* and
1201 Ms6_*23*. **B**. PCR analysis of Girr_Δ*29*-20 and Girr_Δ*29*-25. **C**. Liquid lysis assay of the indicated
1202 phages was carried out as described in Methods. **D**. Amino acid alignment of Girr gp29, NBJ
1203 gp29 and Ms6 gp23 by Clustal Omega. **E**. Plaque assay of Girr_WT, Girr_Δ*29-20*, Girr Δ*29-25*,
1204 NBJ_WT, and NBJ_Δ*29.* Ruler = 1cm. Plaque sizes were determined as described in Methods.
1205 The average plaque diameter +/- standard deviation for 25 plaques is shown.
1206
1207
1208

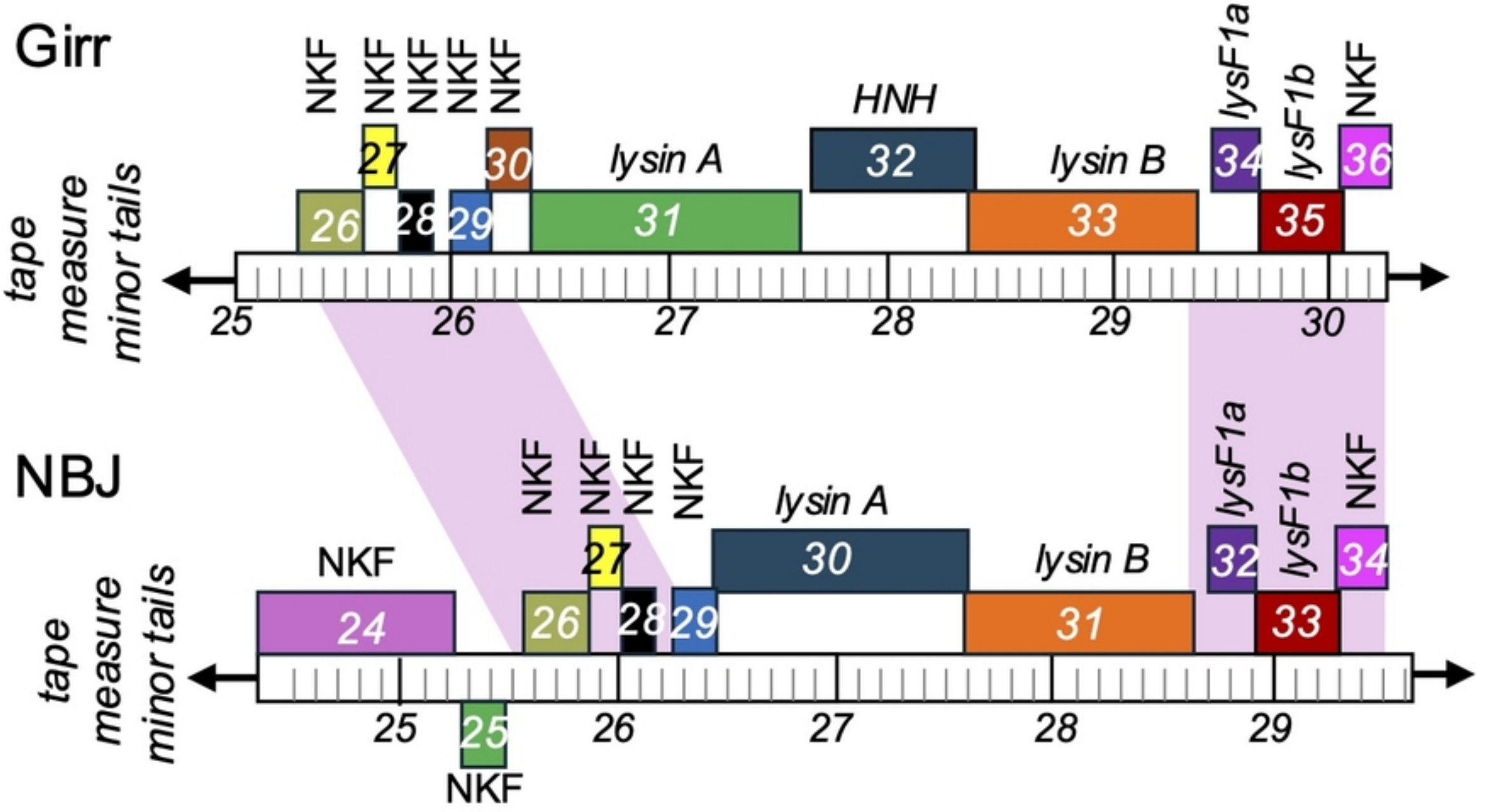
Girr
NKF
NKF
NKF
NKF
NKF
27
30
HNH
32
lysin A
31
lysin B
33
lysF1a
34
lysF1b
35
NKF
36
26
28
29
tape measure minor tails
25
26
27
28
29
30
NBJ
NKF
NKF
NKF
NKF
27
lysin A
30
lysin B
31
lysF1a
32
lysF1b
33
NKF
34
NKF
24
26
28
29
tape measure minor tails
25
25
26
27
28
29
NKF

Figure 1

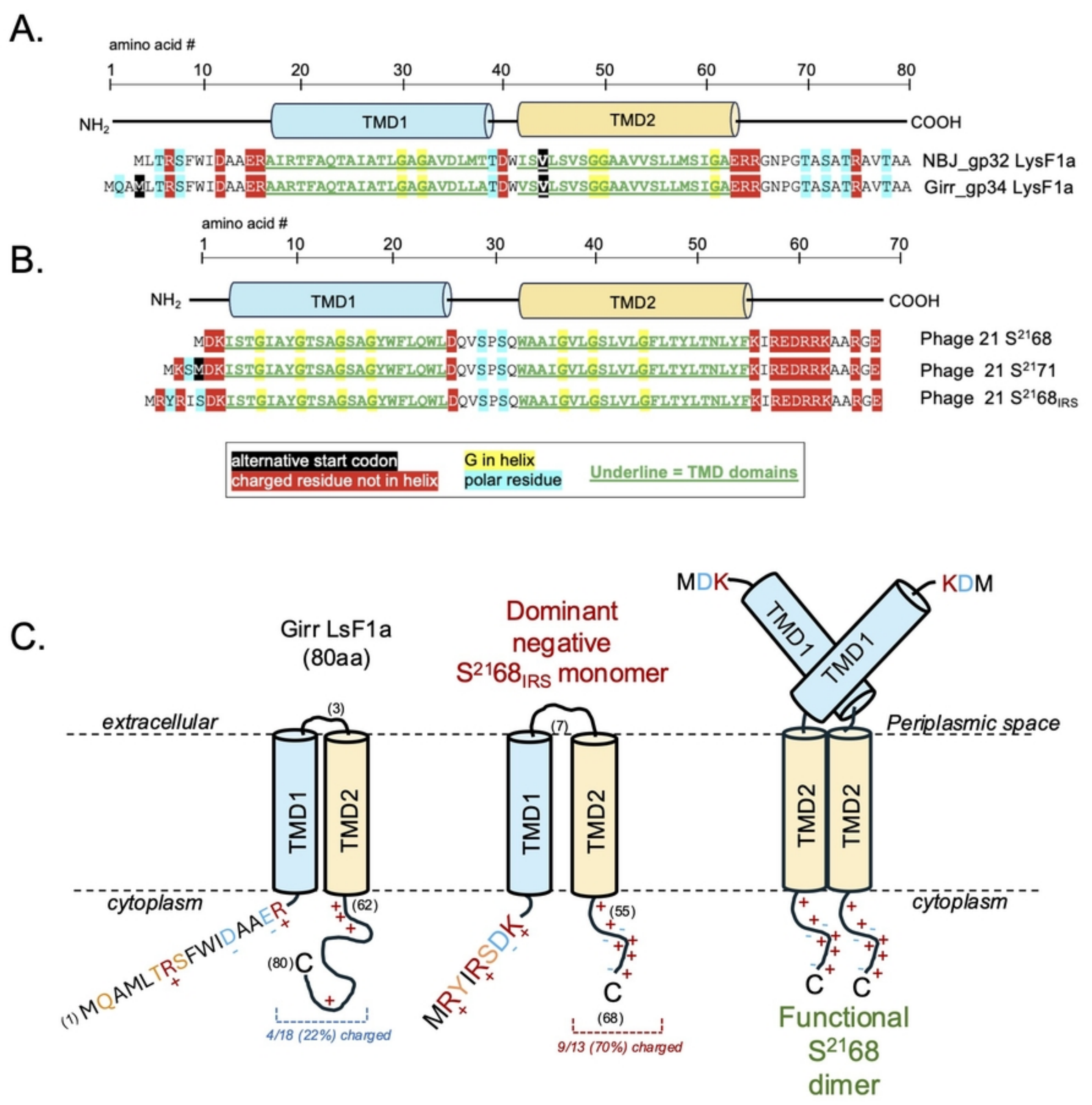
A.
amino acid #
1 10 20 30 40 50 60 70 80
NH2
TMD1
TMD2
COOH
MLTRSFWIDAAERAIRTFAQTAIATLGAGAVDLMTTDWISVLSVSGGAAVVSLLMSIGAERRGNPGTASATRAVTAA NBJ_gp32 LysF1a
MQAMLTRSFWIDAAERAARTFAQTAIATLGAGAVDLLATDWVSVLSVSGGAAVVSLLMSIGAERRGNPGTASATRAVTAA Girr_gp34 LysF1a
B.
amino acid #
1 10 20 30 40 50 60 70
NH2
TMD1
TMD2
COOH
MDKISTGIAYGTSAGSAGYWFLQWLDQVSPSQWAAIGVLGSLVLGFLTYLTNLYFKIREDRRKAARGE Phage 21 S21 68
MKSMDKISTGIAYGTSAGSAGYWFLQWLDQVSPSQWAAIGVLGSLVLGFLTYLTNLYFKIREDRRKAARGE Phage 21 S21 71
MRYRISDKISTGIAYGTSAGSAGYWFLQWLDQVSPSQWAAIGVLGSLVLGFLTYLTNLYFKIREDRRKAARGE Phage 21 S21 68IRS
alternative start codon
charged residue not in helix
G in helix
polar residue
Underline = TMD domains
C.
Girr LsF1a
(80aa)
Dominant
negative
S21 68IRS monomer
MDK
KDM
TMD1
TMD1
extracellular
Periplasmic space
(3)
(7)
TMD1
TMD2
TMD1
TMD2
TMD2
TMD2
cytoplasm
cytoplasm
(62)
(55)
(1) MQAMLTRSFWIDAAER
(80) C
MRYIRSDK
C
(68)
C C
4/18 (22%) charged
9/13 (70%) charged
Functional
S21 68
dimer

Figure 2

A.

1 10 20 30 40 50 60 70 80 90 100 110 120 # amino acids

MIWESVREAVDAAYQPDDGIDLIGLLIIGLPSTIAAIGTGIVGVLTVRGQRKGRERARQIDAKTDEIHEQTVNTHDTNMRDDLDEIRDLVRDGFKQIQRDIGGLREELRTERLERIEGDKRRD Girr gp35 LysF1b

MIWESVREAVDAAYQPDDGIDLIGLLIIGLPSTIAAIGTGIVGVLTVRGQRKGRERARRIDAKTYEIHEQTVNTHDTNMRDDLDEIRDLVRDGFKQIQRDIGGLREELRTERLERIEGDKRRD NBJ gp33 LysF1b

MTGSAVSALPSDWYGLAGLAVVNAAGLLALFMKARGTHKQVANSHSTNLRDDIDGLRDHIVELGRDIGGMRTDVGQLRGEVRDDRTHTHHRFRRIEDKLDELAGRGARESG Waterfoul gp32

MDLISVLALWPYLLPVVAGGAVWAMRRSFASTERVERLENRMTEMETRYASIPGTEDVHEMRLQIAELSGDIRVLSQRVQSFSHQLELLLENAVNRSNS Mu releasin

Green = TMD domain | Basic region after TMD | + Charged | - Charged

B.

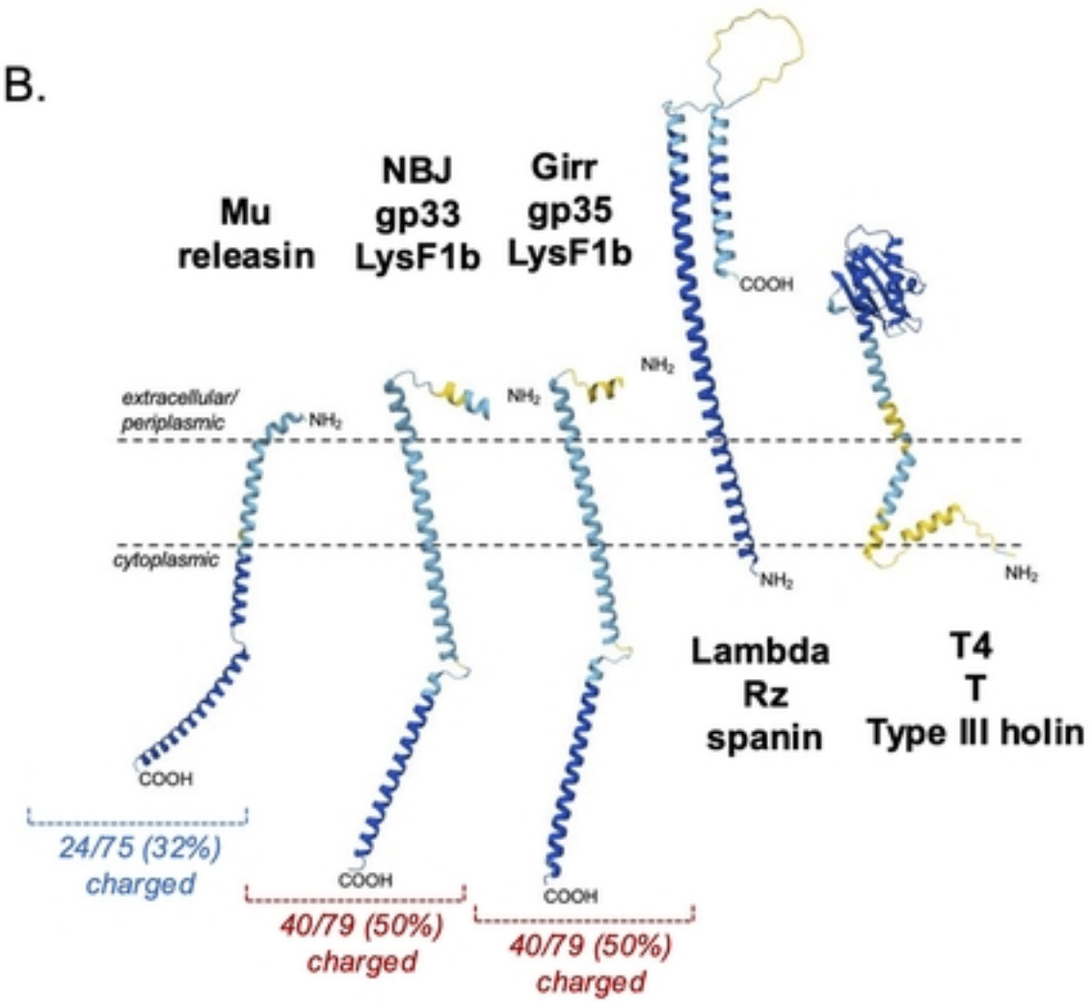

C.

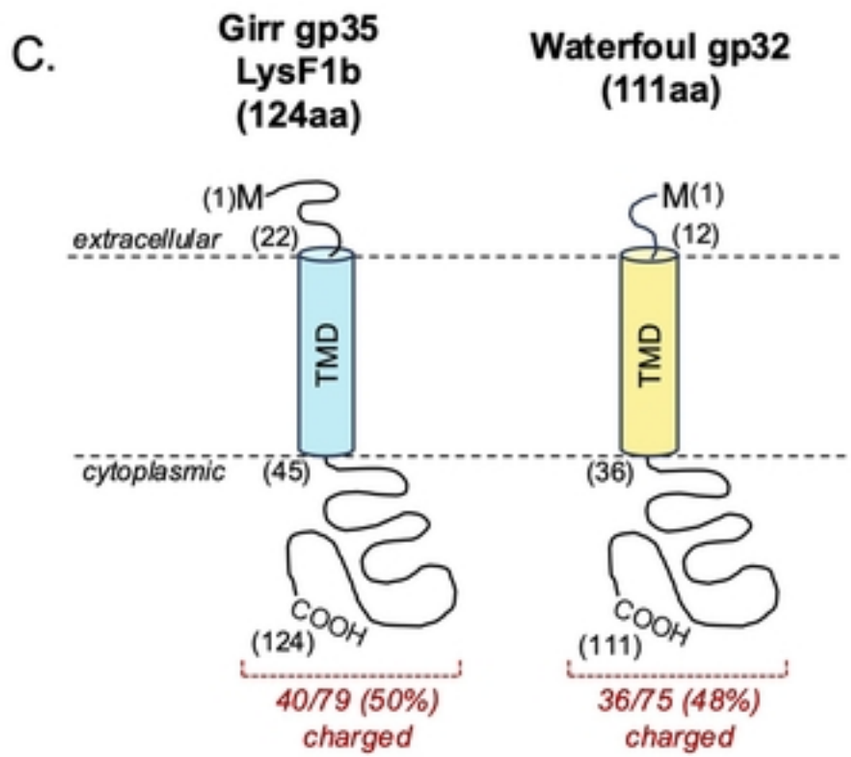

Figure 3

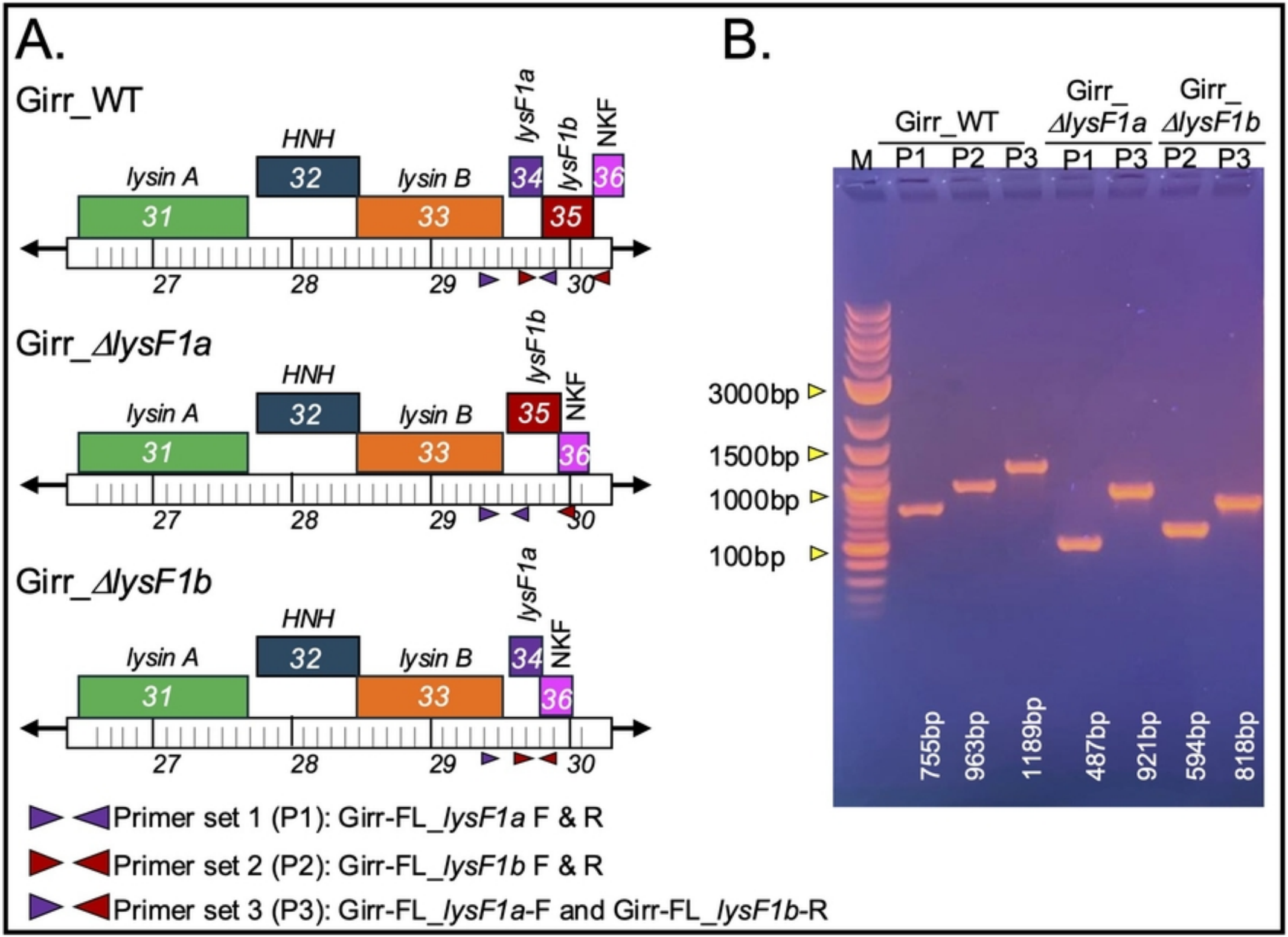
A.
Girr_WT
HNH
lysin A
lysin B
lysF1a
lysF1b
NKF
31
32
33
34
35
36
27
28
29
30
Girr_ΔlysF1a
Girr_ΔlysF1b
B.
Girr_WT
Girr_ΔlysF1a
Girr_ΔlysF1b
M
P1
P2
P3
3000bp
1500bp
1000bp
100bp
755bp
963bp
1189bp
487bp
921bp
594bp
818bp
Primer set 1 (P1): Girr-FL_lysF1a F & R
Primer set 2 (P2): Girr-FL_lysF1b F & R
Primer set 3 (P3): Girr-FL_lysF1a-F and Girr-FL_lysF1b-R

Figure 4

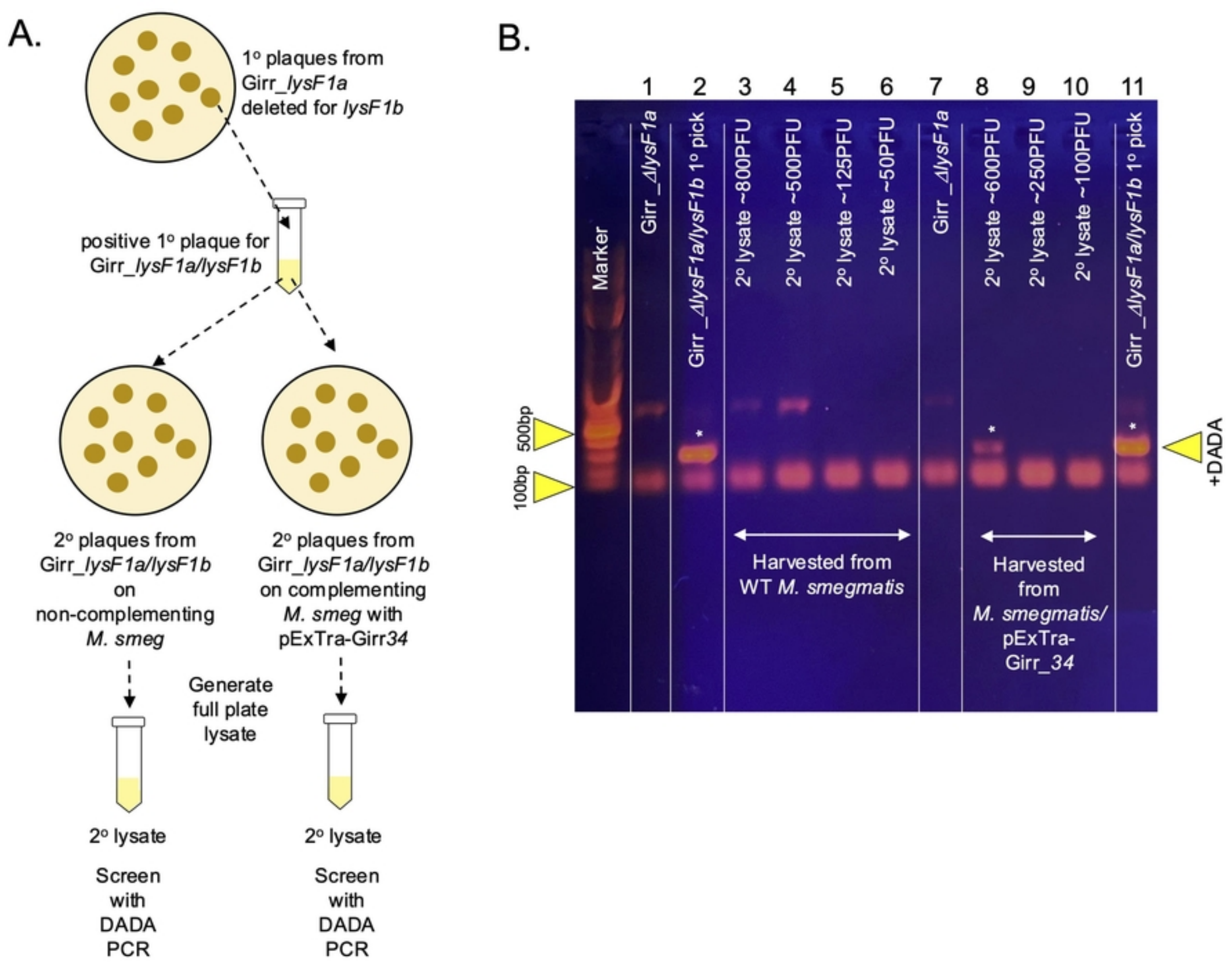
A.
1º plaques from
Girr_lysF1a
deleted for lysF1b
positive 1º plaque for
Girr_lysF1a/lysF1b
2º plaques from
Girr_lysF1a/lysF1b
on
non-complementing
M. smeg
2º plaques from
Girr_lysF1a/lysF1b
on complementing
M. smeg with
pExTra-Girr34
Generate
full plate
lysate
2º lysate
2º lysate
Screen
with
DADA
PCR
Screen
with
DADA
PCR
B.
1 2 3 4 5 6 7 8 9 10 11
Marker
Girr _ΔlysF1a
Girr _ΔlysF1a/lysF1b 1º pick
2º lysate ~800PFU
2º lysate ~500PFU
2º lysate ~125PFU
2º lysate ~50PFU
Girr _ΔlysF1a
2º lysate ~600PFU
2º lysate ~250PFU
2º lysate ~100PFU
Girr _ΔlysF1a/lysF1b 1º pick
500bp
100bp
+DADA
Harvested from
WT M. smegmatis
Harvested
from
M. smegmatis/
pExTra-
Girr_34

Figure 5

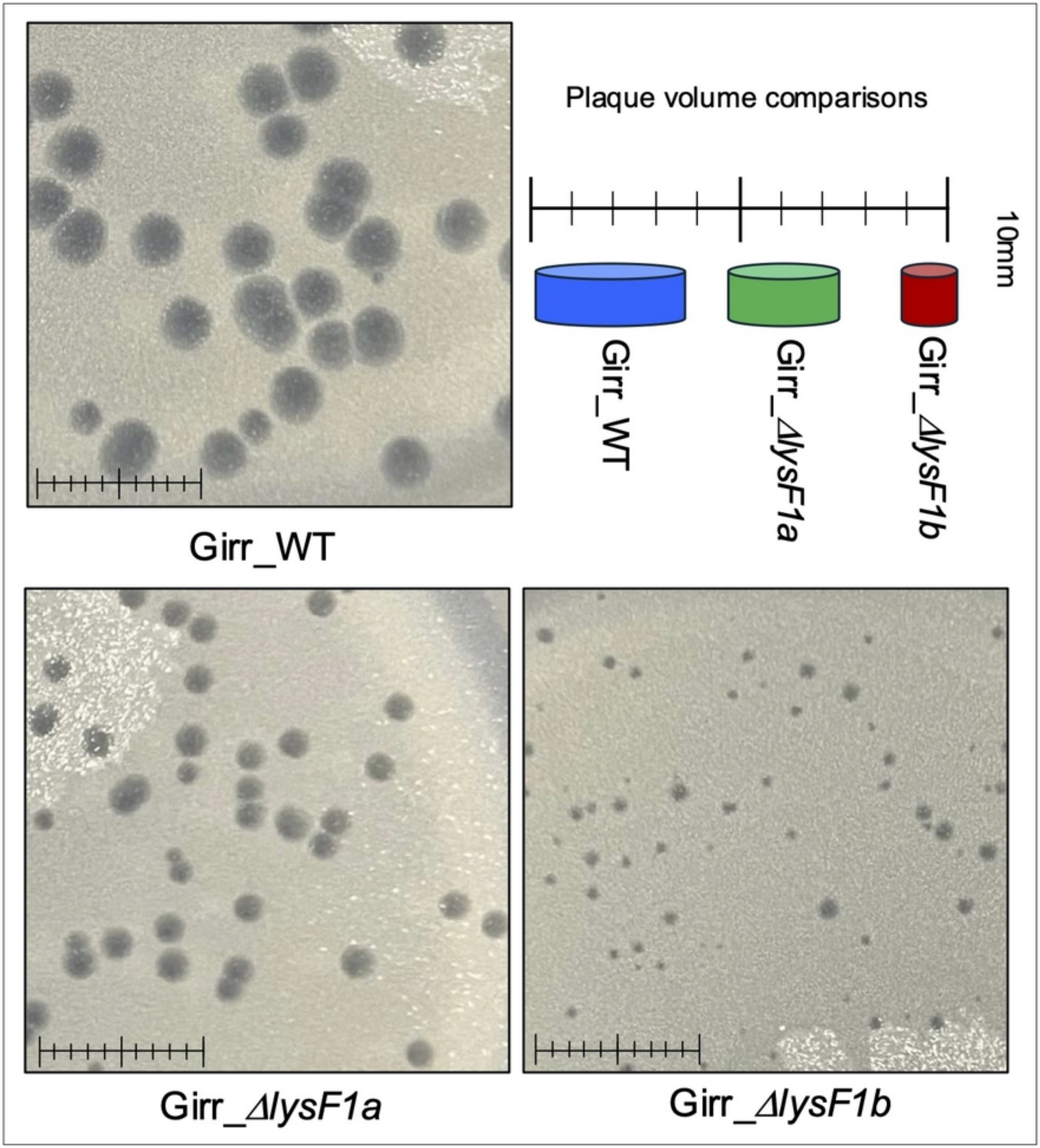
Plaque volume comparisons
10mm
Girr_ΔlysF1b
Girr_ΔlysF1a
Girr_WT
Girr_WT
Girr_ΔlysF1a
Girr_ΔlysF1b

Figure 6

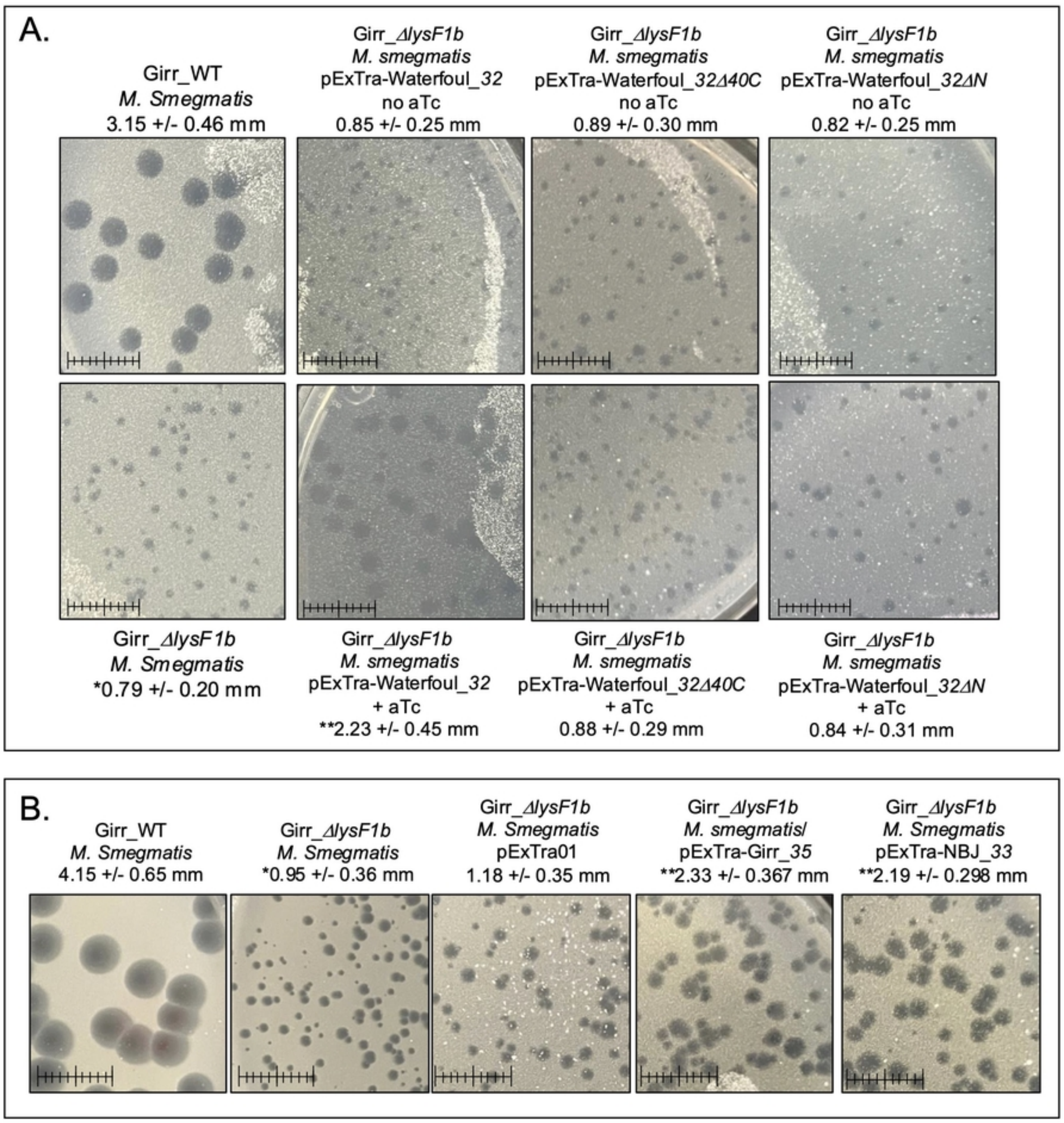
A.
Girr_WT
M. Smegmatis
3.15 +/- 0.46 mm
Girr_ΔlysF1b
M. smegmatis
pExTra-Waterfoul_32
no aTc
0.85 +/- 0.25 mm
Girr_ΔlysF1b
M. smegmatis
pExTra-Waterfoul_32Δ40C
no aTc
0.89 +/- 0.30 mm
Girr_ΔlysF1b
M. smegmatis
pExTra-Waterfoul_32ΔN
no aTc
0.82 +/- 0.25 mm
Girr_ΔlysF1b
M. Smegmatis
*0.79 +/- 0.20 mm
Girr_ΔlysF1b
M. smegmatis
pExTra-Waterfoul_32
+ aTc
**2.23 +/- 0.45 mm
Girr_ΔlysF1b
M. smegmatis
pExTra-Waterfoul_32Δ40C
+ aTc
0.88 +/- 0.29 mm
Girr_ΔlysF1b
M. smegmatis
pExTra-Waterfoul_32ΔN
+ aTc
0.84 +/- 0.31 mm
B.
Girr_WT
M. Smegmatis
4.15 +/- 0.65 mm
Girr_ΔlysF1b
M. Smegmatis
*0.95 +/- 0.36 mm
Girr_ΔlysF1b
M. Smegmatis
pExTra01
1.18 +/- 0.35 mm
Girr_ΔlysF1b
M. smegmatis/
pExTra-Girr_35
**2.33 +/- 0.367 mm
Girr_ΔlysF1b
M. Smegmatis
pExTra-NBJ_33
**2.19 +/- 0.298 mm

Figure 7

Girr_WT
M. Smegmatis
4.56 +/- 0.65 mm

Girr_*ΔlysF1a*
M. Smegmatis
pExTra-Girr*34* + *aTc*
**4.15 +/- 0.55 mm

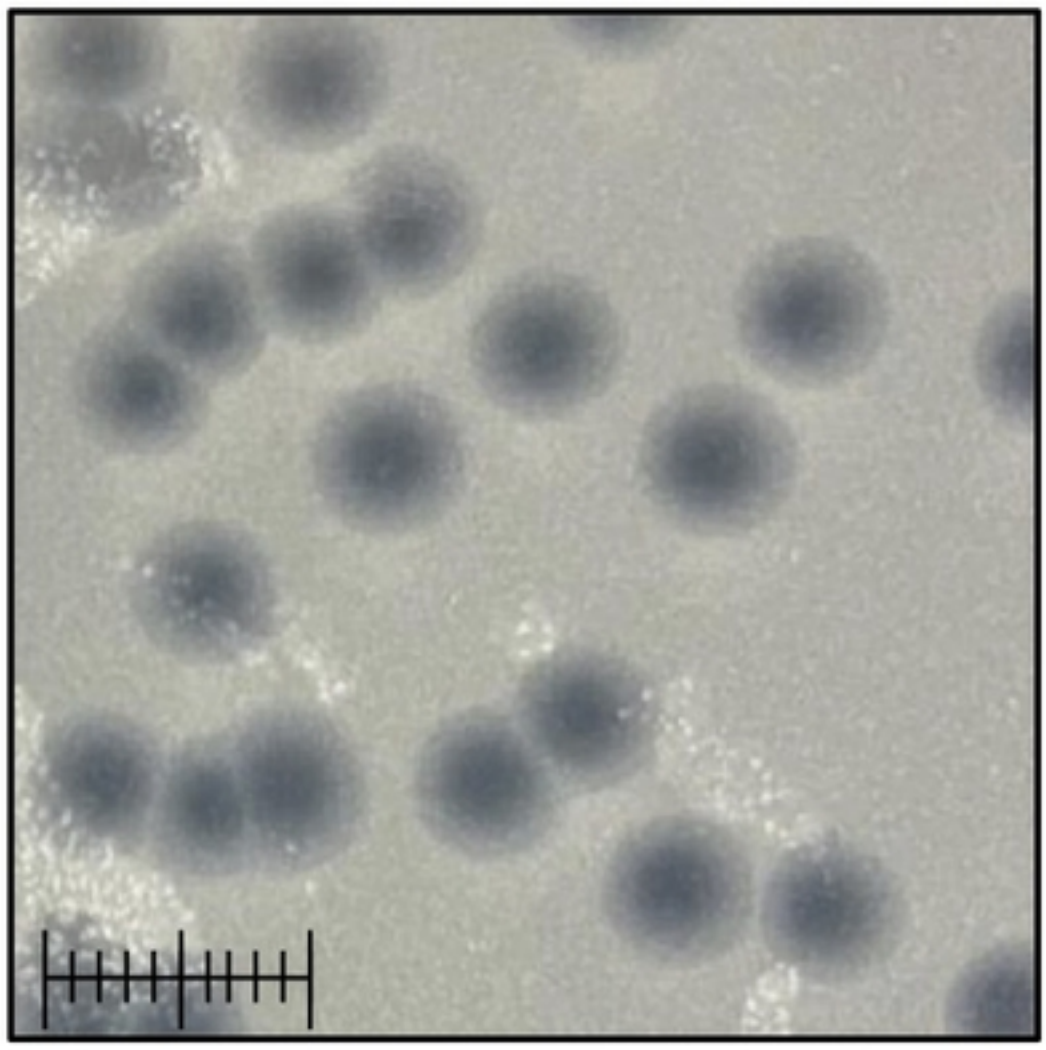

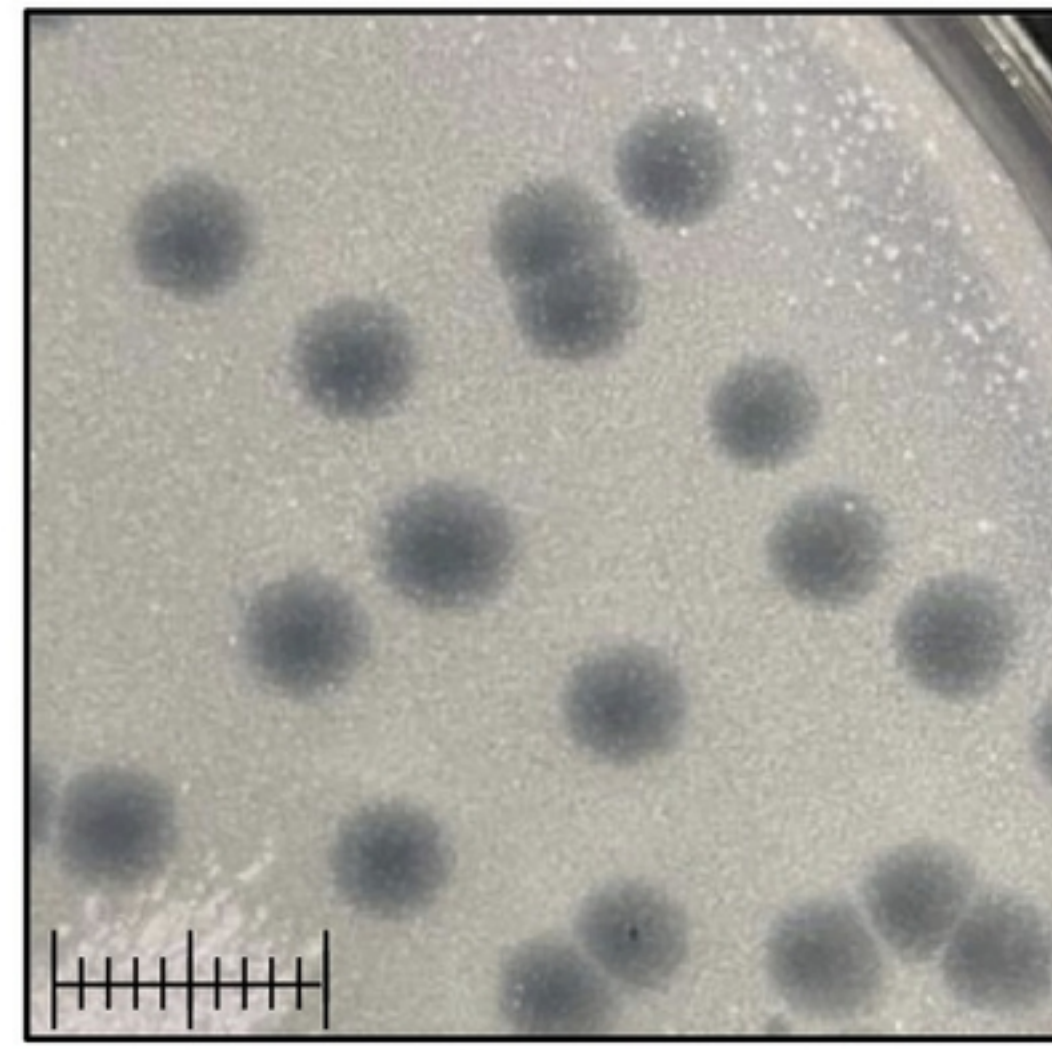

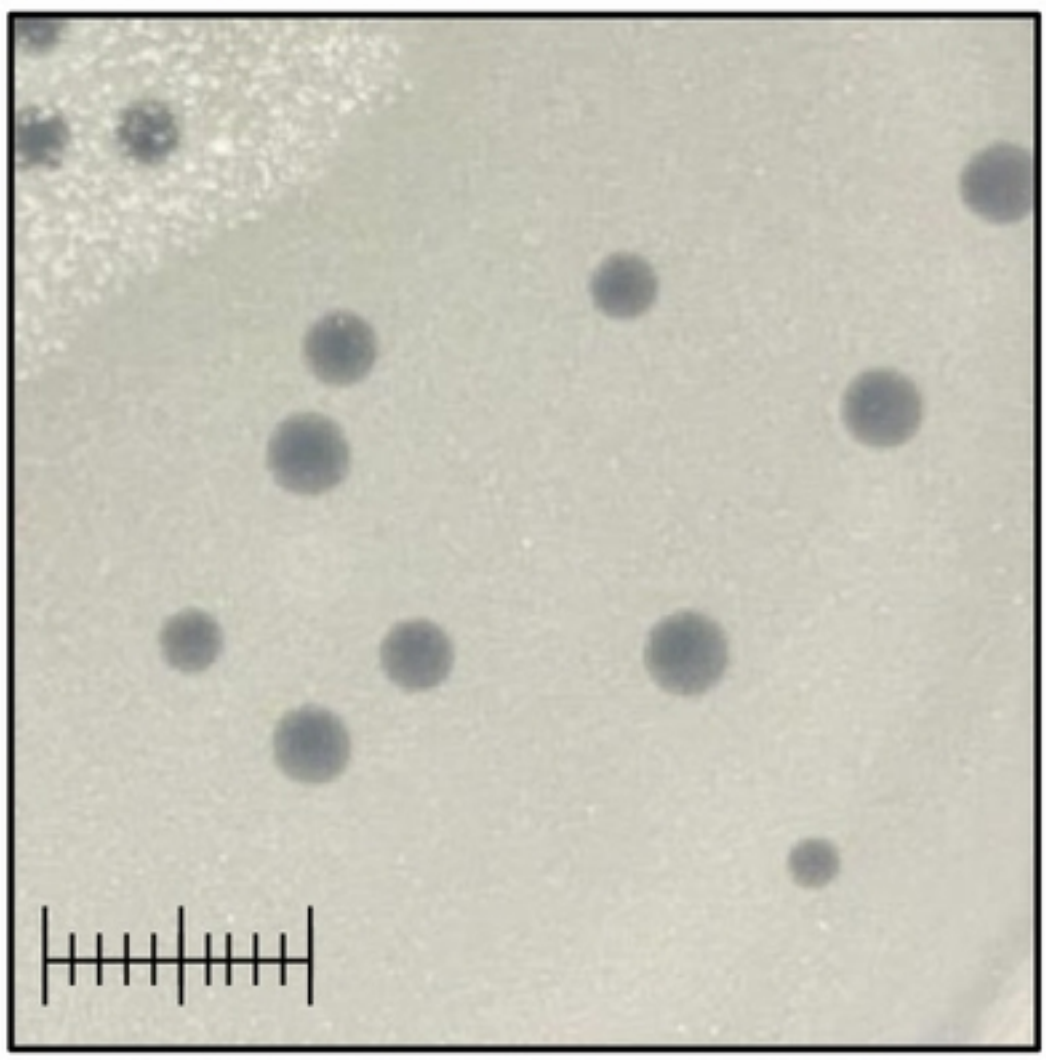

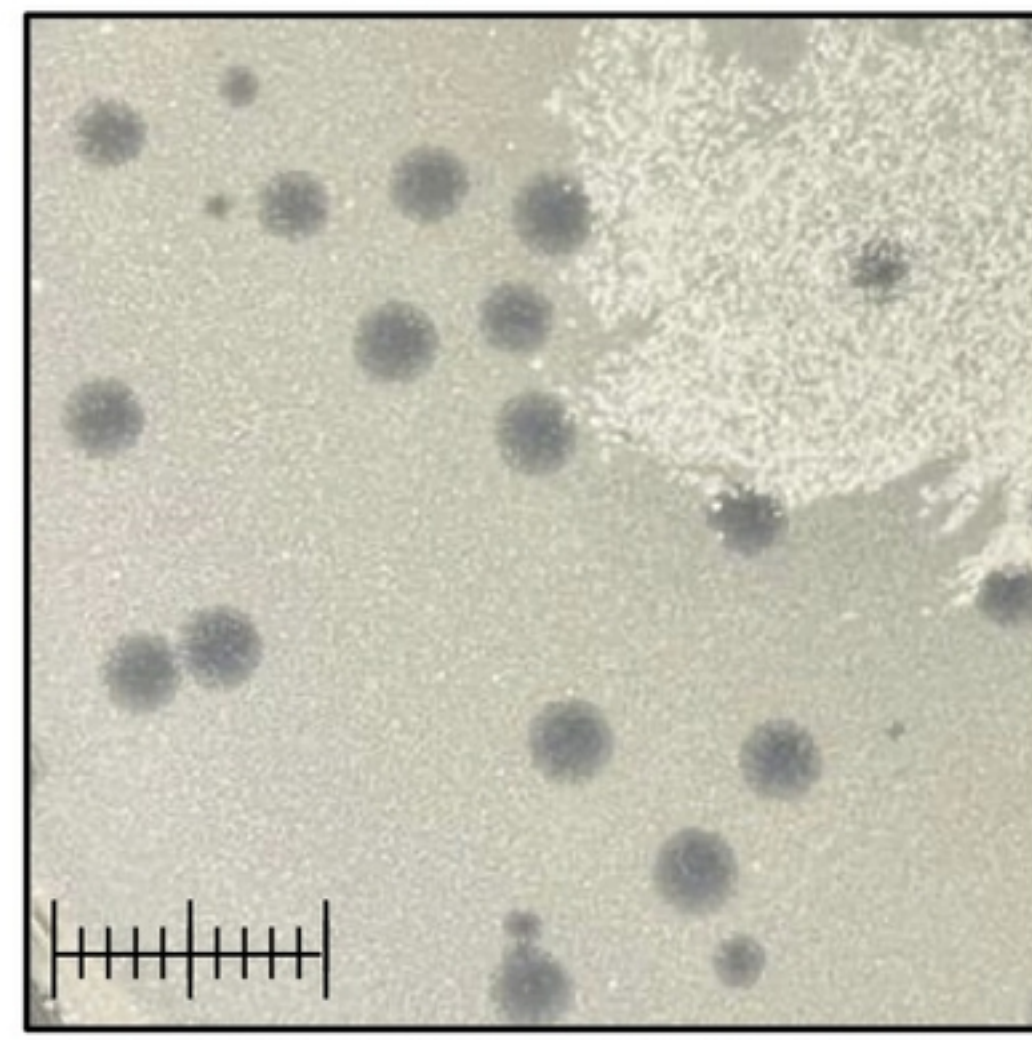

Girr_*ΔlysF1a*
M. Smegmatis
*2.79 +/- 0.55mm

Girr_*ΔlysF1a*
M. Smegmatis
pExTra-Girr*34 no aTc*
2.83 +/- 0.353 mm

Figure 8

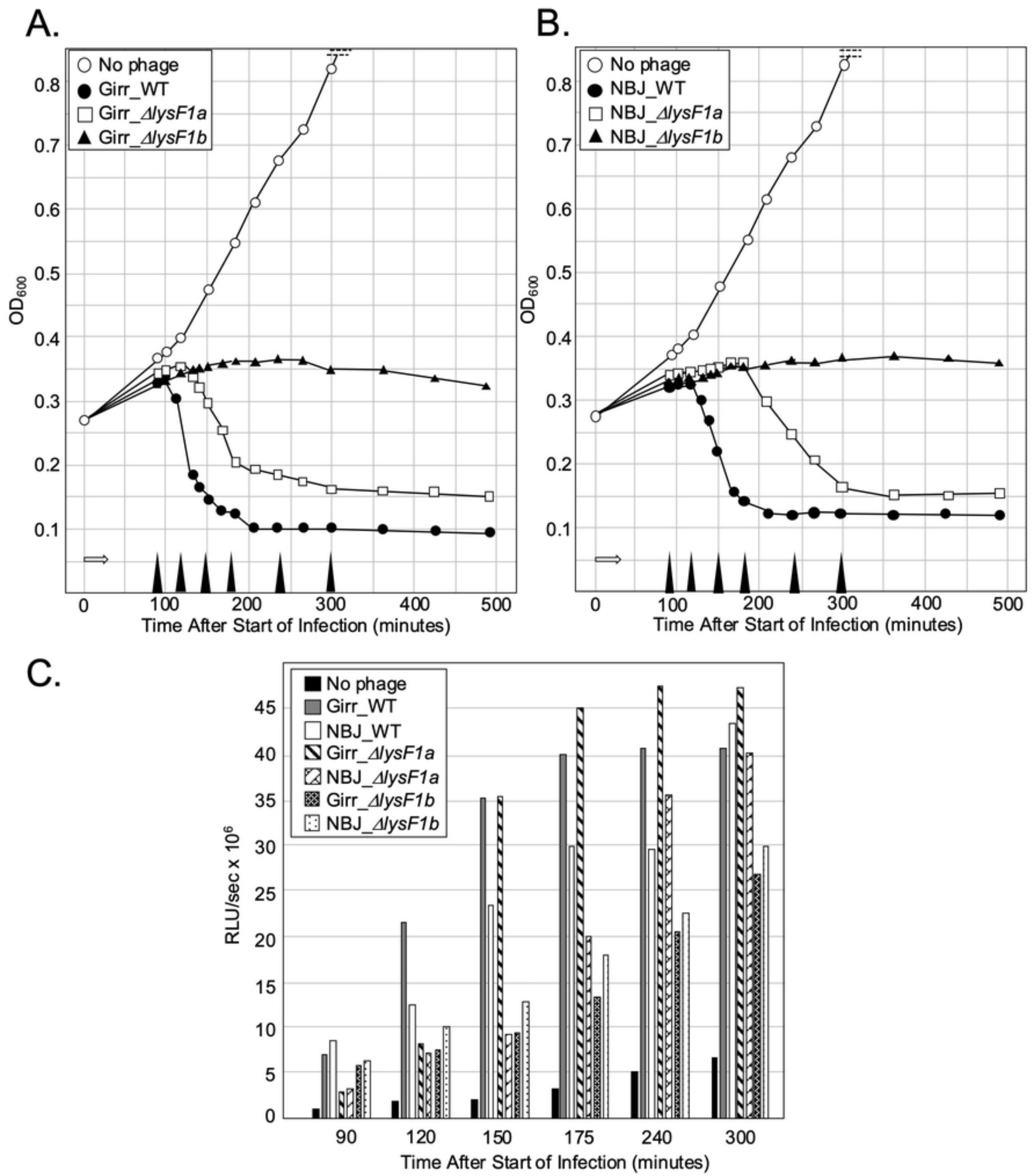
A.
No phage
Girr_WT
Girr_ΔlysF1a
Girr_ΔlysF1b
OD600
0.8
0.7
0.6
0.5
0.4
0.3
0.2
0.1
0
100
200
300
400
500
Time After Start of Infection (minutes)
B.
No phage
NBJ_WT
NBJ_ΔlysF1a
NBJ_ΔlysF1b
OD600
0.8
0.7
0.6
0.5
0.4
0.3
0.2
0.1
0
100
200
300
400
500
Time After Start of Infection (minutes)
C.
No phage
Girr_WT
NBJ_WT
Girr_ΔlysF1a
NBJ_ΔlysF1a
Girr_ΔlysF1b
NBJ_ΔlysF1b
RLU/sec x 10^6
45
40
35
30
25
20
15
10
5
0
90
120
150
175
240
300
Time After Start of Infection (minutes)

Figure 9

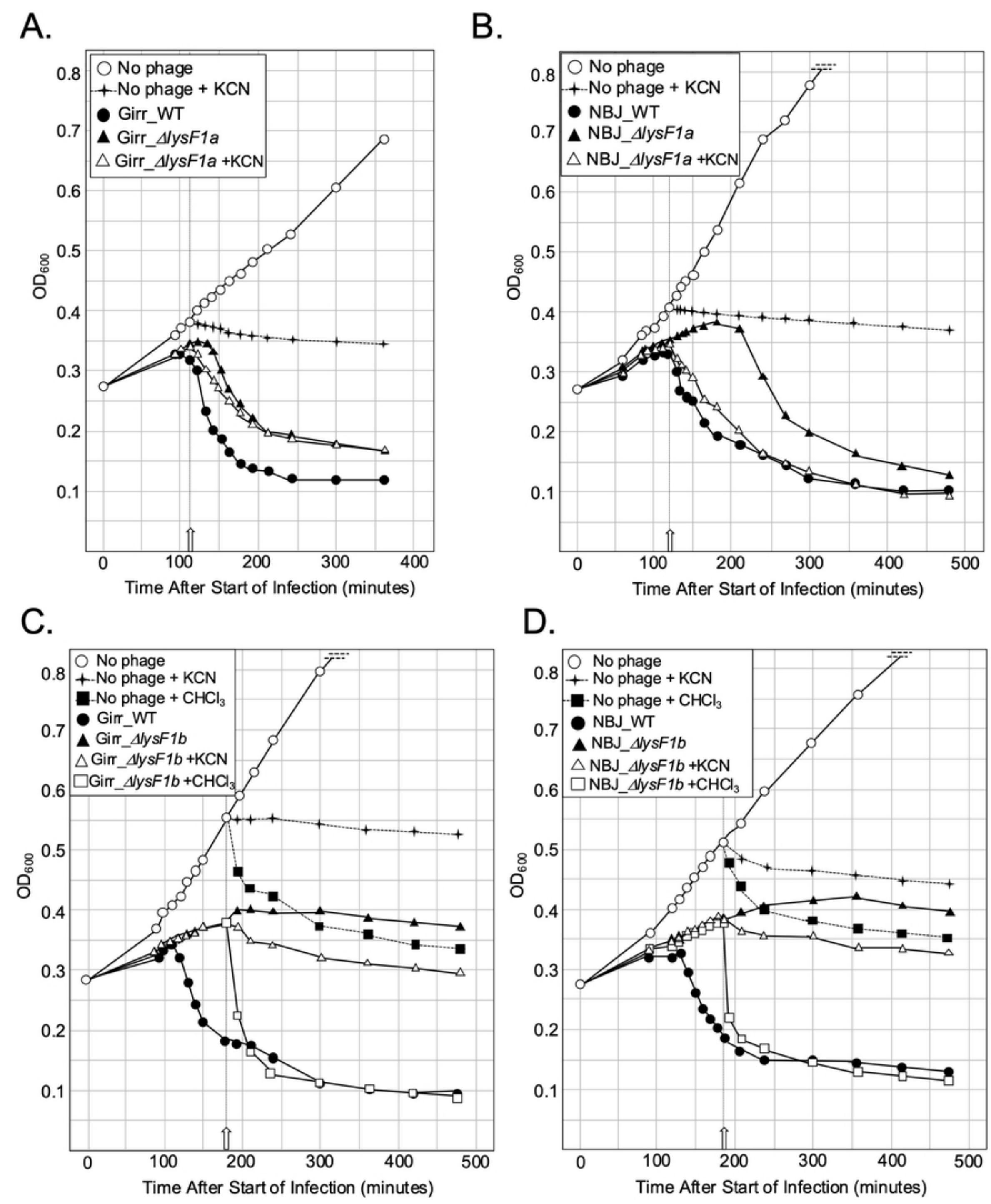
A.
No phage
No phage + KCN
Girr_WT
Girr_ΔlysF1a
Girr_ΔlysF1a +KCN
OD600
Time After Start of Infection (minutes)
B.
No phage
No phage + KCN
NBJ_WT
NBJ_ΔlysF1a
NBJ_ΔlysF1a +KCN
OD600
Time After Start of Infection (minutes)
C.
No phage
No phage + KCN
No phage + CHCl3
Girr_WT
Girr_ΔlysF1b
Girr_ΔlysF1b +KCN
Girr_ΔlysF1b +CHCl3
OD600
Time After Start of Infection (minutes)
D.
No phage
No phage + KCN
No phage + CHCl3
NBJ_WT
NBJ_ΔlysF1b
NBJ_ΔlysF1b +KCN
NBJ_ΔlysF1b +CHCl3
OD600
Time After Start of Infection (minutes)

Figure 10

A.

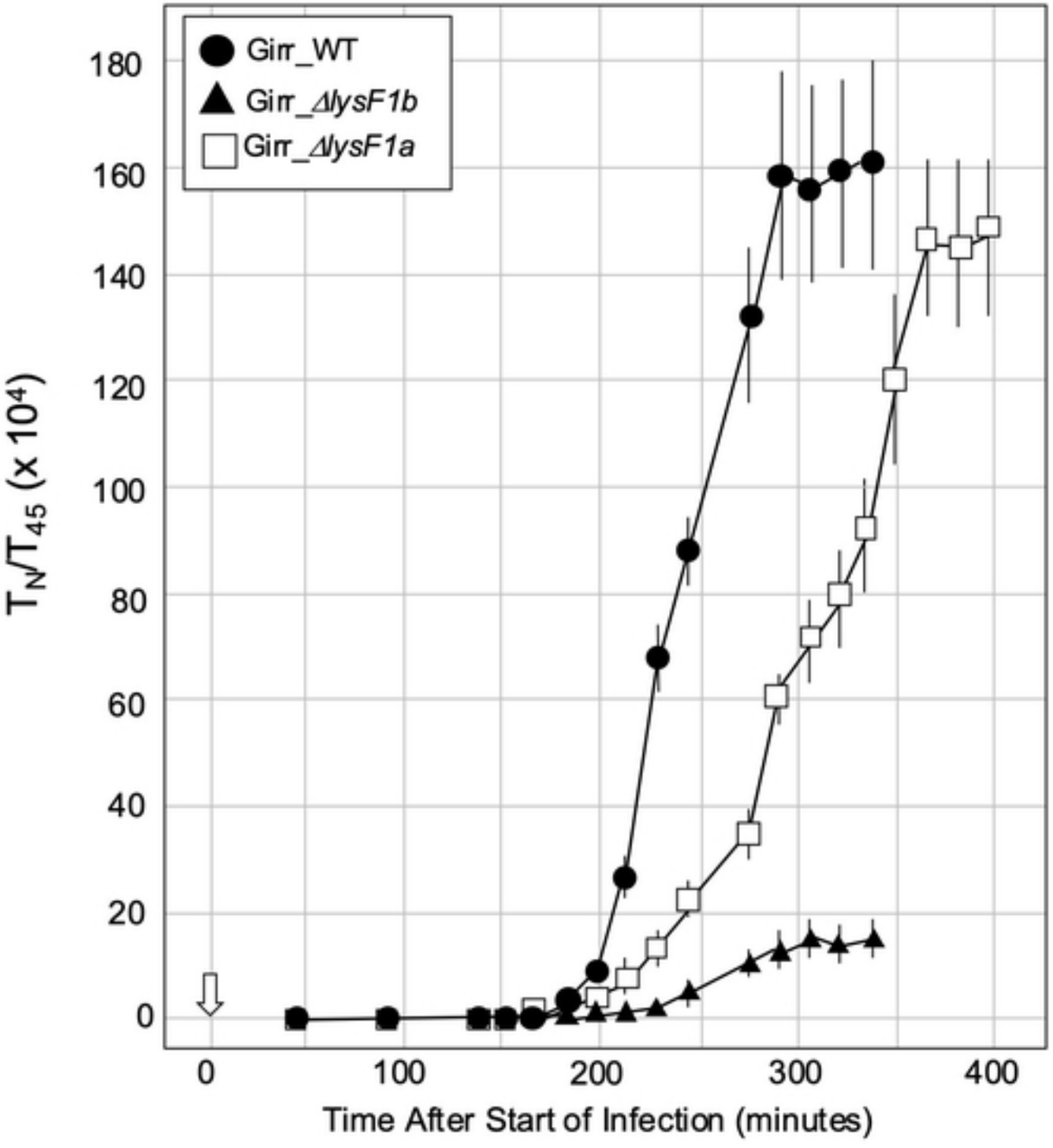

B.

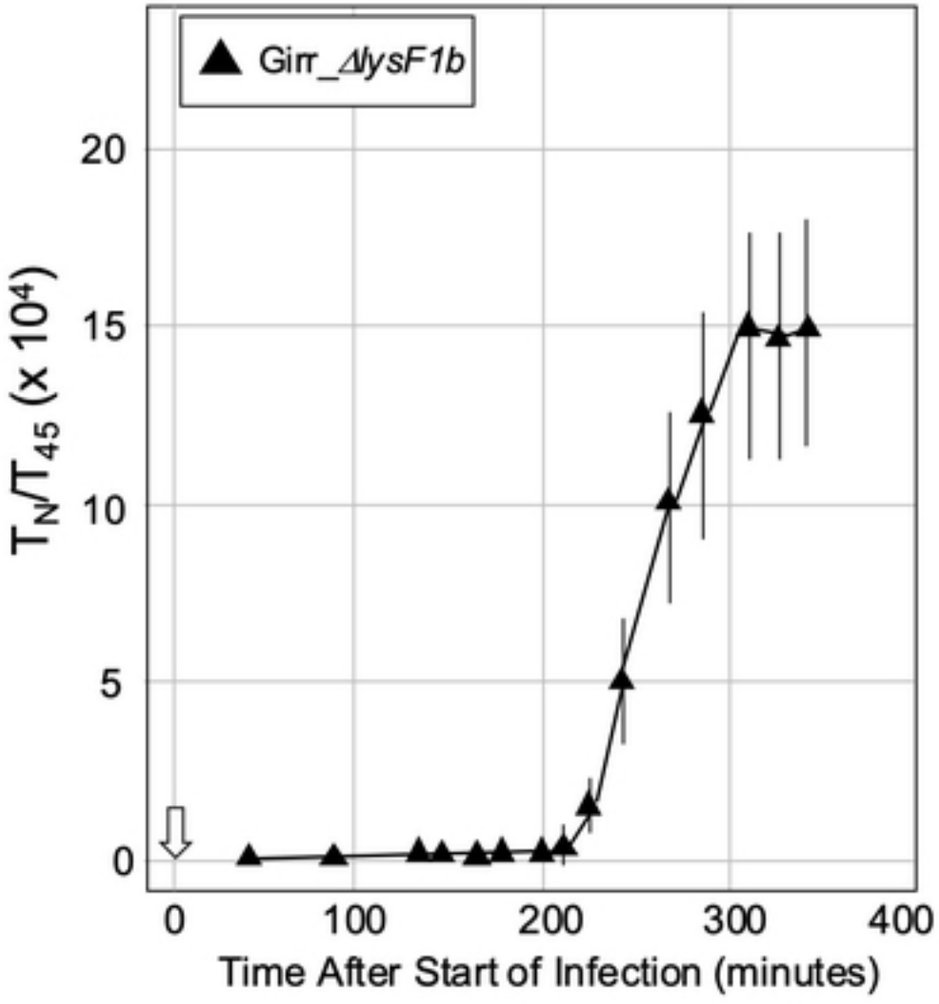

C.

phage	Burst Size PFU/cell
Girr_WT	277 +/- 81
Girr_*ΔlysF1a*	255 +/- 75
Girr_*ΔlysF1b*	*29.2 +/- 36

*statistically significant from WT phage $p<0.0001$.

Figure 11

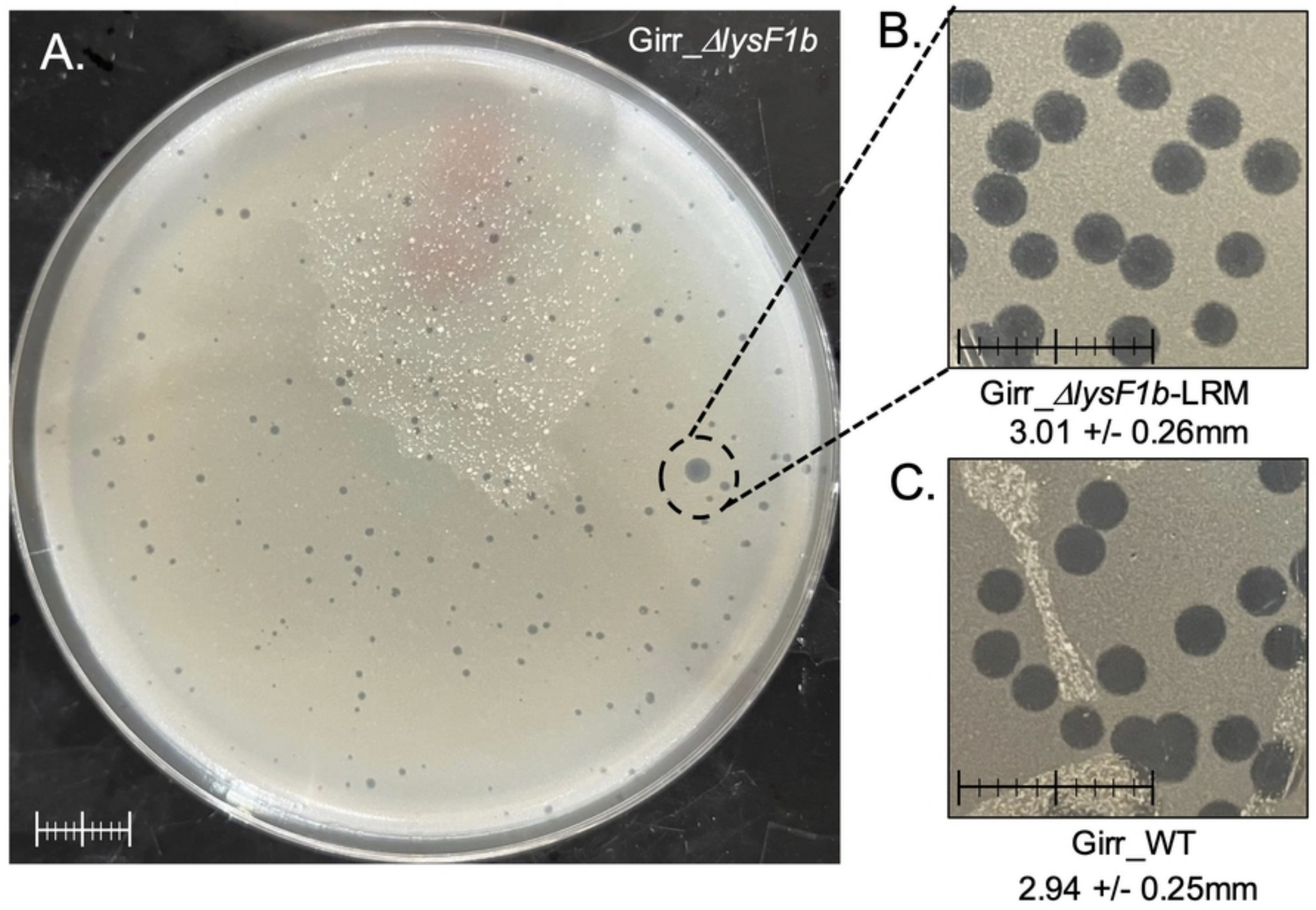
A.
Girr_ΔlysF1b
B.
Girr_ΔlysF1b-LRM
3.01 +/- 0.26mm
C.
Girr_WT
2.94 +/- 0.25mm

Figure 12

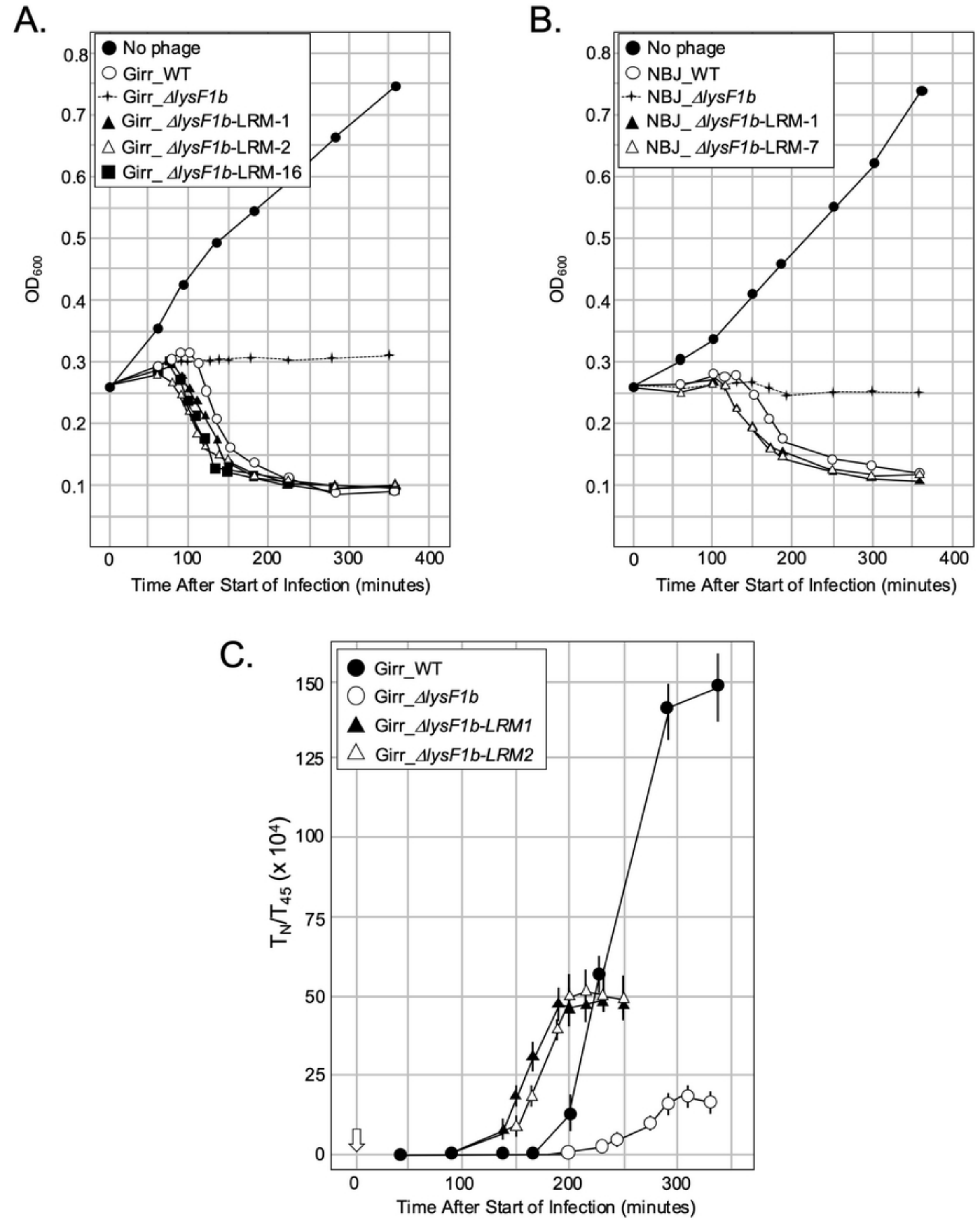
A.
No phage
Girr_WT
Girr_ΔlysF1b
Girr_ ΔlysF1b-LRM-1
Girr_ ΔlysF1b-LRM-2
Girr_ ΔlysF1b-LRM-16
OD600
Time After Start of Infection (minutes)
B.
No phage
NBJ_WT
NBJ_ΔlysF1b
NBJ_ ΔlysF1b-LRM-1
NBJ_ ΔlysF1b-LRM-7
OD600
Time After Start of Infection (minutes)
C.
Girr_WT
Girr_ΔlysF1b
Girr_ΔlysF1b-LRM1
Girr_ΔlysF1b-LRM2
TN/T45 (x 10^4)
Time After Start of Infection (minutes)

Figure 13

A.

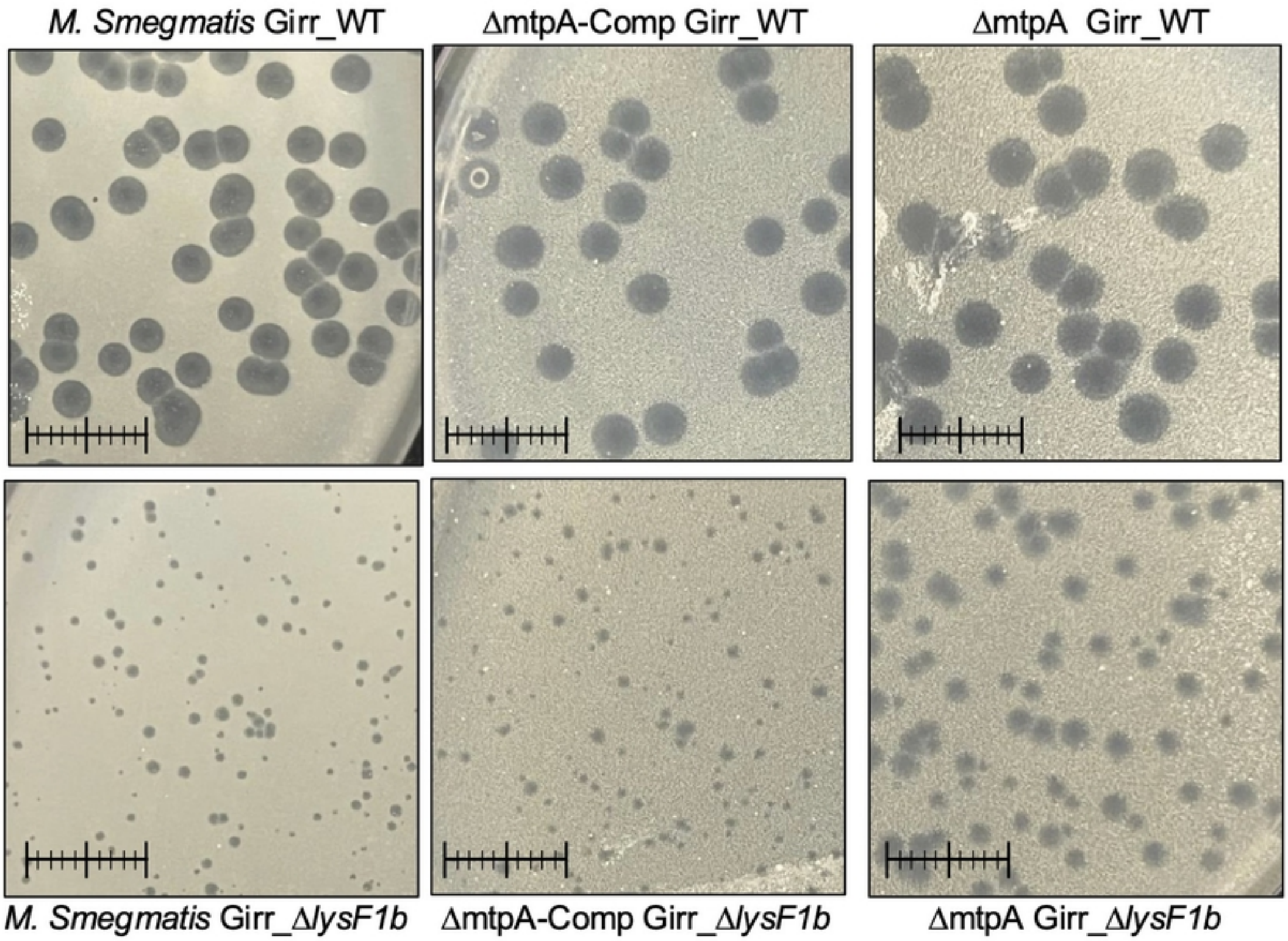
M. Smegmatis Girr_WT
ΔmtpA-Comp Girr_WT
ΔmtpA Girr_WT
M. Smegmatis Girr_ΔlysF1b
ΔmtpA-Comp Girr_ΔlysF1b
ΔmtpA Girr_ΔlysF1b

B.

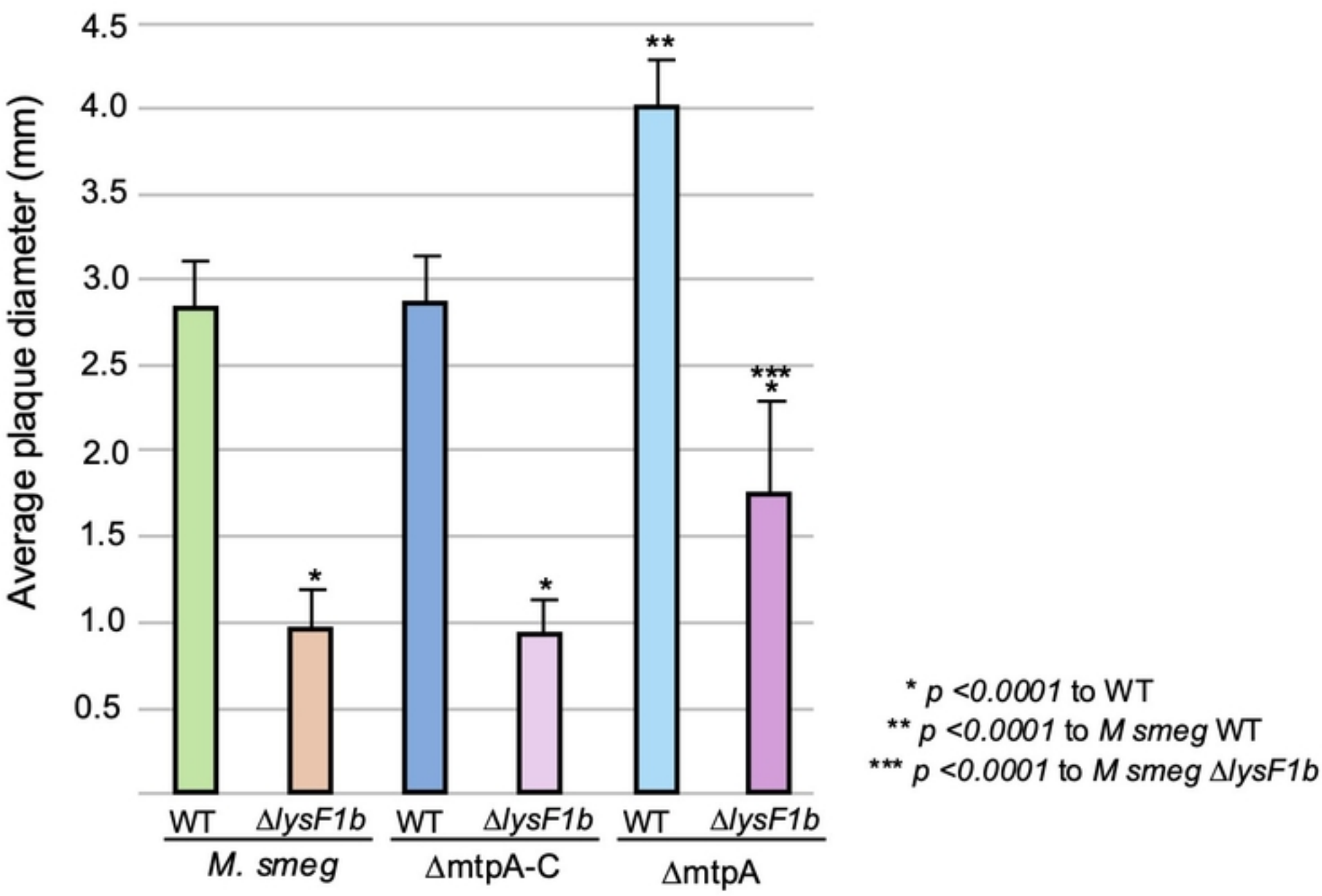
Average plaque diameter (mm)
4.5
4.0
3.5
3.0
2.5
2.0
1.5
1.0
0.5
**
***
*
*
*
WT
ΔlysF1b
WT
ΔlysF1b
WT
ΔlysF1b
M. smeg
ΔmtpA-C
ΔmtpA
* p <0.0001 to WT
** p <0.0001 to M smeg WT
*** p <0.0001 to M smeg ΔlysF1b

Figure 14

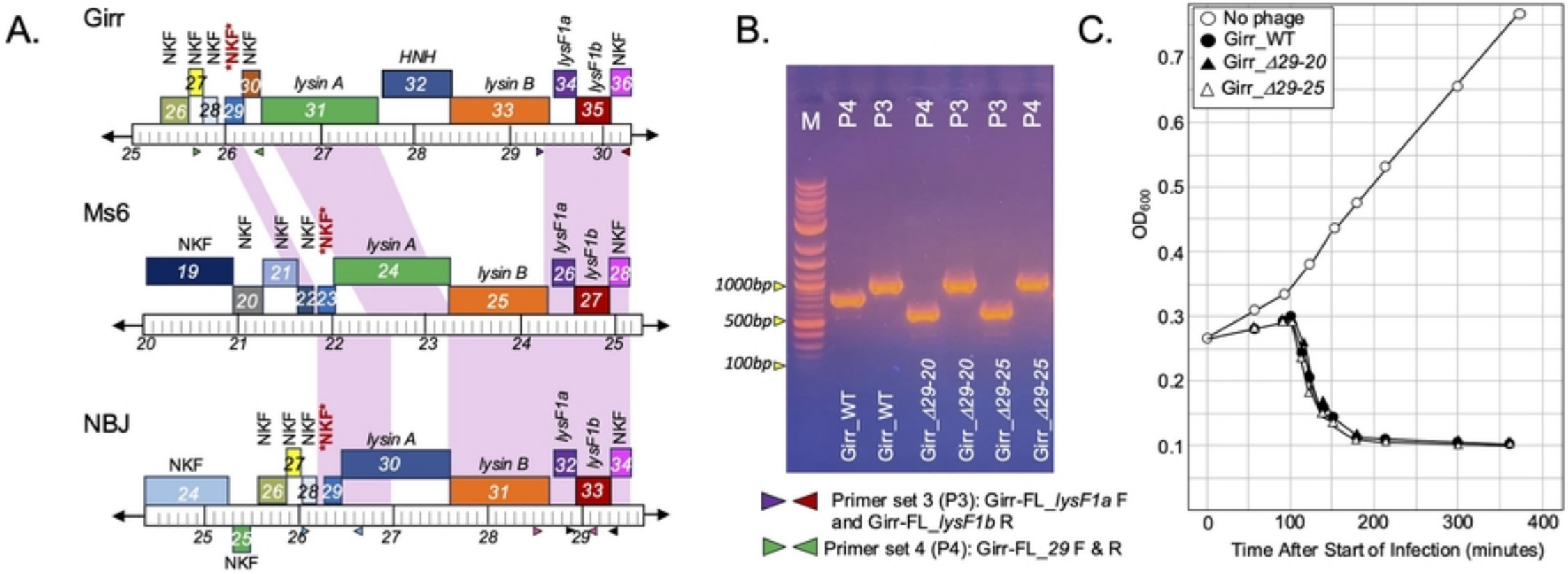

D.

```
Girr_29   MDRLGIILLKLLGPLADRIADRIADRITENLPDLSDLDDQIVAKLPDLTNLPEQVINIIGRLPRFPFLLGGKP
Ms6_23    MDRLGIVLLKLFGPLADRIADRIADRIAENLPDLSNLDDQIVAKLPDLTNLPAQVMDIIDSALRSIPVLGGILGSKR
NBJ_29    MDRLGIILLKLFGPLADRIADRIADRITENLPDLSNLDDQIVAKLPDLTNLPAQVMDIIDGALRSIPVLGGILGSKR
```

E.

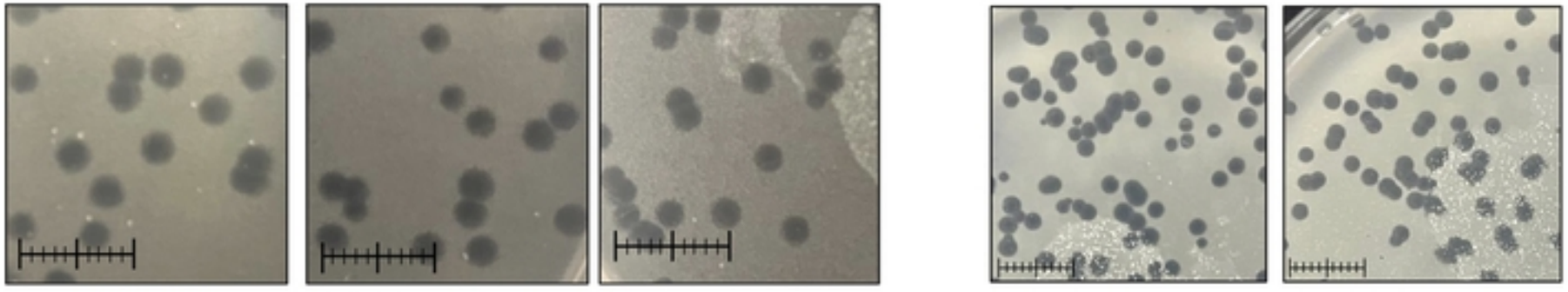

Girr_WT 3.11 +/- 0.12 nm | Girr_Δ29-20 2.98 +/- 0.16 nm | Girr_Δ29-25 3.02 +/- 0.14 nm | NBJ_WT 2.25 +/- 0.25 nm | NBJ_Δ29 2.15 +/- 0.09 nm

Figure 15